https://doi.org/10.5194/tc-2020-302
Preprint. Discussion started: 27 October 2020

The Cryosphere Discussions
Open Access
EGU

Continuous monitoring of surface water vapour isotopic compositions at Neumayer Station III, East Antarctica

Saeid Bagheri Dastgerdi[1], Melanie Behrens[1], Jean-Louis Bonne[1], Maria Hörhold[1], Gerrit Lohmann[1], Elisabeth Schlosser[2,3], and Martin Werner[1]

[1]Alfred Wegener Institute Helmholtz-Center for Polar and Marine Research Bremerhaven, Bremerhaven, Germany
[2]Department of Atmospheric and Cryospheric Sciences, University of Innsbruck, Innsbruck, Austria
[3]Austrian Polar Research Institute, Vienna, Austria

Correspondence: Saeid Bagheri Dastgerdi (saeid.bagheri@awi.de)

Abstract. In this study, the first fully-continuous monitoring of water vapour isotopic composition at Neumayer Station III, Antarctica, during the two-year period from February 2017 to January 2019 is presented. Seasonal and synoptic-scale variations of both stable water isotopes $H_2^{18}O$ and HDO are reported, and their link to variations of key meteorological variables are analysed. Changes in local temperature and humidity are the main drivers for the variability of $\delta^{18}O$ and δD in vapour at Neumayer Station III, both on seasonal and shorter time scales. In contrast to the measured $\delta^{18}O$ and δD variations, no seasonal cycle in the Deuterium excess signal d–excess in vapour is detected. However, a rather high uncertainty of measured d–excess values especially in austral winter limits the confidence of this finding. Overall, the d–excess signal shows a stronger inverse correlation with humidity than with temperature, and this inverse correlation between d–excess and humidity is stronger for the cloudy-sky conditions than for clear-sky conditions during summertime. Back trajectory simulations performed with the FLEXPART model show that seasonal and synoptic variations of $\delta^{18}O$ and δD in vapour coincide with changes in the main sources of water vapour transported to Neumayer Station. In general, moisture transport pathways from the east lead to higher temperatures and more enriched $\delta^{18}O$ values in vapour, while weather situations with southerly winds lead to lower temperatures and more depleted $\delta^{18}O$ values. However, for several occasions, $\delta^{18}O$ variations linked to wind direction changes were observed, which were not accompanied by a corresponding temperature change. Comparing isotopic compositions of water vapour at Neumayer Station III and snow samples taken in the vicinity of the station reveals almost identical slopes, both for the $\delta^{18}O$–δD relation and for the temperature–$\delta^{18}O$ relation.

1 Introduction

During the last decades, Antarctic ice cores have been proven to be one of the most important climate archives. They have enabled a detailed climate reconstruction on glacial-interglacial time scales over the last 800,000 years (EPICA Members, 2004; Jouzel et al., 2007) and are furthermore the only climate archive which allows direct measurements of past greenhouse gas changes (Petit et al., 1999; Siegenthaler et al., 2005; Loulergue et al., 2008; Lüthi et al., 2008). Recent Antarctic ice core records also allow studying the phasing of climate changes and the linkage between northern and southern polar regions in an unprecedented way (Buizert et al., 2015).

https://doi.org/10.5194/tc-2020-302
Preprint. Discussion started: 27 October 2020


The Cryosphere Discussions
Open Access
EGU

Measurements of stable water isotopes (here given in the usual $\delta^{18}O$ and δD notation) are crucial for the analyses of ice core records. Since the pioneering work of Dansgaard (1964), Lorius and Merlivat (1975), and others, stable water isotopes in Antarctic ice cores have been used as a proxy to reconstruct past temperature changes. Recent intensive sampling campaigns on various expeditions and locations in Antarctica have increased our knowledge about the present-day variability of $\delta^{18}O$ and δD at different spatial scales (Masson-Delmotte et al., 2008; Münch et al., 2016; Casado et al., 2017). Furthermore, measurements of stable water isotopes of Antarctic deep ice cores revealed insights into temperature changes on glacial-interglacial time scales (e.g. Jouzel and Merlivat, 1984).

Although the fundamental physical processes, which link the isotopic fractionation processes during precipitation formation in clouds, the condensation temperature, and the surface temperature at the precipitation location, are well understood (Jouzel and Merlivat, 1984), the quantification of this temperature–isotope relationship remains difficult. While early studies have assumed an equality between the observed modern spatial temperature–isotope relation and the temporal relation required to reconstruct past temperatures (Petit et al., 1999), it has become clear that the spatial relationship differs from the temporal relationship (e.g. Sime et al., 2009). A proper isotope paleothermometer calibration is hampered by different processes, like changes in the temperature inversion strength (Salamatin et al., 1998), changes in the seasonality or intermittency of snowfall events (e.g. Masson-Delmotte et al., 2006), changes in the glacial ice sheet height (Werner et al., 2018), or changes in the origin and transports pathways of moisture to Antarctica (e.g. Masson-Delmotte et al., 2011; Sime et al., 2013).

Another process that might alter the $\delta^{18}O$ and δD value in Antarctic ice cores is the post depositional exchange of water isotopes between vapour and the surface snow layer. Since a few years, new commercial laser instruments have enabled continuous in situ measurements of atmospheric water vapour isotopes with high sampling frequency (Kerstel et al., 1999; Lee et al., 2005). Recent studies on the Greenland ice sheet have reported an isotopic exchange between the near-surface vapour and the surface snow between precipitation events (Madsen et al., 2019; Steen-Larsen et al., 2014). For the location of Dome C, East Antarctica, Casado et al. (2018) also concluded from a combination of precipitation and snow pit samples that the water isotopic composition of ice cores is not solely governed by the δ-signal in precipitation. So far, only a few observational studies directly monitoring vapour isotopic composition have been performed in Antarctica. They have all been limited to relatively short measurement periods during the austral summer season. Ritter et al. (2016) carried out continuous measurements of water vapour isotopes at Kohnen Station, East Antarctica, during the austral summer season 2013–2014. Their isotopic data show a similar pattern for different days with a strong diurnal cycle. Casado et al. (2016) performed measurements of water vapour isotopes in the austral summer season 2014–2015 at Concordia Station on the East Antarctic plateau. They found two different patterns of diurnal isotope cycles. One pattern showed almost stable water vapour isotopes, while the second pattern illustrated a very high correlation between water vapour isotopes, humidity, and temperature. Both studies by Ritter et al. (2016) and Casado et al. (2016) focused their analyses on the diurnal cycle and showed that the isotopic composition in Antarctic snow changes during periods without precipitation. Bréant et al. (2019) measured the isotopic composition of water vapour during a 40-day period in the austral summer season 2016–2017 at the Dumont d'Urville station in Adélie Land. They also report clear diel cycles of temperature, humidity and isotopic composition. Their measurements and analyses showed that low $\delta^{18}O$ and high d–excess values in vapour at Dumont d'Urville could be linked to katabatic winds, which transport strongly depleted

https://doi.org/10.5194/tc-2020-302
Preprint. Discussion started: 27 October 2020


The Cryosphere Discussions

vapour from the inner East Antarctic ice sheet to the station. In contrast, Kurita et al. (2016) used shipboard observations of the isotopic composition of water vapour between Australia and the East Antarctic coast to analyse the influence of marine air intrusion on temporal isotopic variations in vapour at Syowa Station, East Antartica, during the austral summer seasons 2013–14 and 2014–15. They showed that northerly winds, associated with cyclones, might push marine air with isotopically enriched moisture into the East Antarctic inland.

Here, we report measurements of the isotopic composition of vapour from the Neumayer Station III, Antarctica, performed over a full two-year period between February 2017 and January 2019. To our knowledge, this is the first study continuously monitoring Antarctic vapour during all seasons of the year. The primary purpose of this study is a characterization of water vapour and related isotope changes at Neumayer Station III on annual, seasonal, and sub-seasonal time scales. This dataset can form the basis for further process studies on the potential vapour–snow exchange of stable water isotopes in Antarctica. In addition, it can be used as a new dataset to evaluate the capability of global and regional climate models with explicit water isotope diagnostics (e.g. Risi et al., 2010; Werner et al., 2011; Pfahl et al., 2012) to correctly simulate mean isotopic composition and temporal variations of $\delta^{18}O$ and δD in Antarctic water vapour.

This paper is organized in five chapters. The following Chapter 2 explains our instrumental setup to perform continuous measurements of water vapour and its isotopic composition at Neumayer Station III. In this chapter other meteorological datasets and methods used in this study are described, too. In Chapter 3, we report on the performed measurements and analyses, which focus on the relation between changes of water isotopes in vapour and several key meteorological variables on different time scales. Chapter 4 discusses our results in a broader context and compares them to the reported isotope variations in vapour at other Antarctic locations. The results of this study will be summarized in the final Chapter 5.

2 Methods and data

2.1 Study site

Neumayer Station III (simply called Neumayer Station, hereafter) is a German Antarctic research station, located at 70°40′S, 8°16′W (Fig. 1) run by the Alfred Wegener Institute (AWI), Helmholtz-Centre for Polar and Marine Research. AWI has provided continuous synoptic observations since 1981, first at the former Georg-von-Neumayer Station (70°37′S, 8°22′W) until March 1992, thereafter at Neumayer Station II (70°39′S, 8°15′W) and since February 2009 at Neumayer Station III (70°40′S, 8°16′W) (König-Langlo and Loose, 2007). The station is situated on the 200-meter thick Ekström ice shelf approximately 42 m above sea level. This ice shelf has a homogeneous, flat surface slightly sloping upwards to the south (Klöwer et al., 2013). While the shortest distance from the station to the ice shelf edge amounts to 6.2 km (towards ENE), the base is moving with the ice shelf towards the open sea in the north (16 km distance) at about 200 meters per year (König-Langlo and Loose, 2007). Close to Neumayer Station, the sea ice extent has a minimum in February and a maximum in September and the coastlines are usually ice-free for parts of the summer (König-Langlo and Loose, 2007).

Like most coastal Antarctic stations, weather and climate at Neumayer Station are characterized by relatively high wind speeds, with an annual mean value of 8.7 $m\ s^{-1}$ (1-sigma standard deviation: $\pm 6.1 m\ s^{-1}$). Two main wind directions are

https://doi.org/10.5194/tc-2020-302
Preprint. Discussion started: 27 October 2020

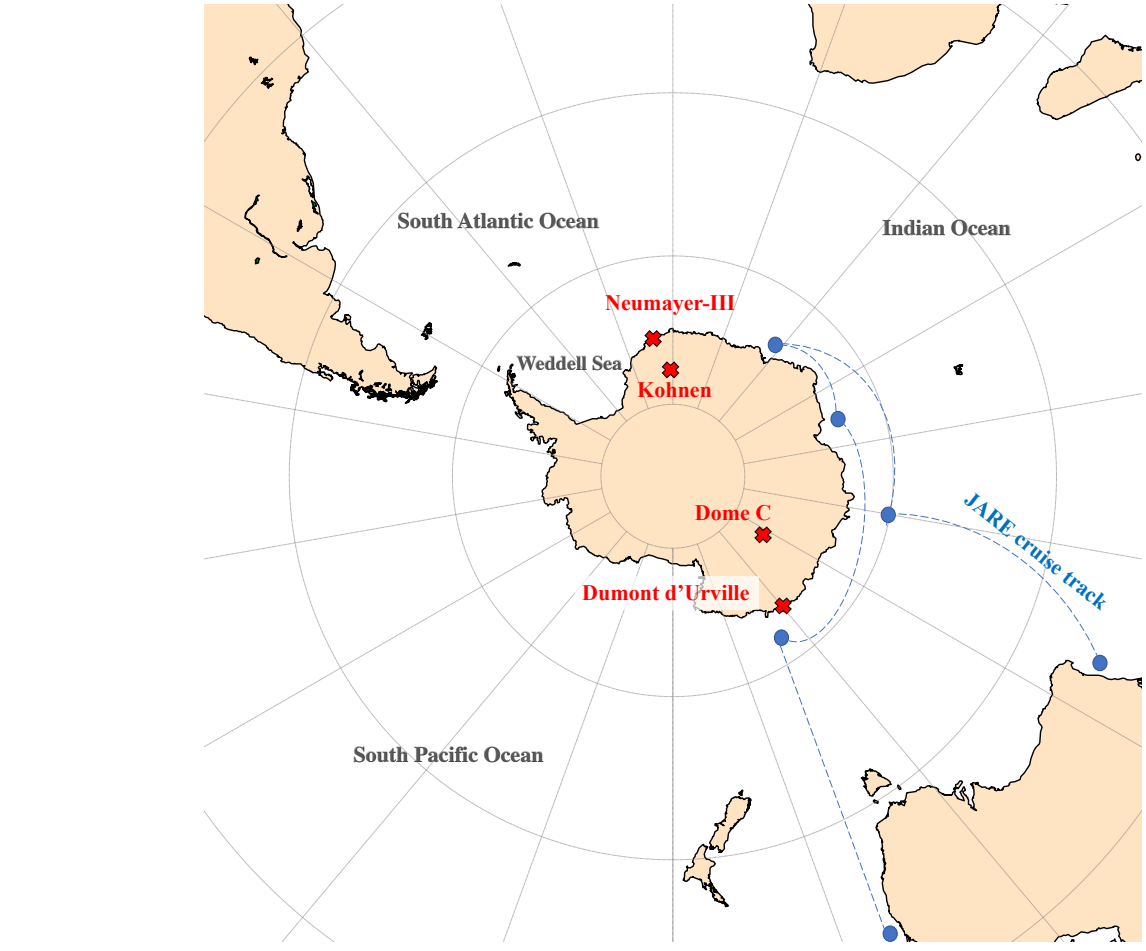

Figure 1. Map of Antarctica. The location of our study (Neumayer III) and other studies which provided continuous water vapour isotopic measurements in Antarctica (Ritter et al., 2016; Casado et al., 2016; Bréant et al., 2019) are shown in red colour and JARE cruise track related to Kurita et al. (2016) is shown in blue colour.

found. The prevailing wind direction is east, caused by the passage of cyclones north of the Antarctic coast in the circumpolar trough. Easterly storms are common, with wind speeds up to approximately 40 $m\ s^{-1}$. The second, less frequent, typical wind direction is south to southwest, caused by a mixture of weak katabatic and synoptic influence, with typical wind speeds below 10 $m\ s^{-1}$ (König-Langlo and Loose, 2007; Rimbu et al., 2014).

Depending on the snow surface conditions, drifting or blowing snow can start at relatively low wind speeds between 6 $m\ s^{-1}$ and 12 $m\ s^{-1}$. At Neumayer Station, drifting or blowing snow is reported in 40 % of all visual observations (König-Langlo and Loose, 2007). Direct quantification of precipitation is almost impossible due to the influence of drifting and blowing snow. The mean annual accumulation has been determined glaciologically and amounts to approximately 340mm w.e. (water equivalent). The mean annual temperature at Neumayer Station (since 1981) is $-16.10°C$ ($\pm 1.05°C$). Since the beginning of

https://doi.org/10.5194/tc-2020-302
Preprint. Discussion started: 27 October 2020

the measurements in 1981 no significant temporal trend in air temperature has been observed (also shown by Medley et al., 2018).

2.2 Meteorological observations

In this study, temperature, humidity, wind speed, and wind direction data, measured 50 meters away from the station at 2-meter height above the surface, are used. We use meteorological observations at a resolution of 1 hour for the period February 2017-January 2019. To identify specific days with extreme high or low temperature, we determine multi-year daily temperature averages over the 38-year period from 1981 to 2018 (König-Langlo, 2017) and calculate the daily temperature anomaly at Neumayer Station. A day is considered as a warm (cold) event, when its temperature anomaly is higher (lower) than one standard deviation above (below) the mean.

2.3 Water vapour isotopic observations

In January 2017, a PICARRO L2140-i cavity ring-down spectroscopy analyser (simply named Picarro analyser, hereafter), has been installed in a lab room at Neumayer Station. The Picarro analyser is running continuously and measures the injected water vapour content and its isotopic composition approximately every two seconds. For our analyses, the data are merged to hourly mean values, if not stated otherwise.

For the largest time of the year, wind at Neumayer Station blows from easterly, southerly, or southwesterly directions. Therefore, the air inlet for the vapour measurements is located on eastern side of the roof towards the mean wind direction and at its southern end to avoid exhaust gases. Apart from the time when the instrument is calibrated (see below), ambient air is constantly transported by an electrical pump from the rooftop to the Picarro analyser. During the calibration, to avoid keeping old air inside the tube, the pump continues sucking the air from the rooftop without sending it to the Picarro analyser. The whole inlet tube (approx. 10m long) is constantly heated to approx. 65°C to avoid any condensation of vapour within the inlet tube.

Part of the instrumental setup is a custom-made calibration system using three different isotopic water standards (liquid), with $\delta^{18}O$ values of -6.07 ± 0.1 ‰, -25.33 ± 0.1 ‰, and -43.80 ± 0.1 ‰. δD values of the standards (water liquid) are -43.73 ± 1.5 ‰, -195.21 ± 1.5 ‰, and -344.57 ± 1.5 ‰. The chosen isotope values of the standards cover the whole range of expected isotope values in vapour at Neumayer Station (from -17 ‰ to -54 ‰ for $\delta^{18}O$ and from -120 ‰ to -404 ‰ for δD) during the course of a year. Isotope standards are provided in liquid form, and a bubbler system similar to the one described in Steen-Larsen et al. (2013) is used for vapourizing and measuring the standards. For safety reasons, two independent cooler boxes with two isotopic standards, each, are installed, and the isotope standard with a $\delta^{18}O$ value of -25.33 ‰ is measured in both cooler boxes. The boxes are held at a constant temperature of 17°C and air and water temperatures inside each bubbler system are constantly logged to determine the isotopic value of the vapour stemming from the liquid standards during the calibration measurements.

For calibrating our isotope measurements, the calibration protocol developed by Steen-Larsen et al. (2013) and Bonne et al. (2014) has been applied and modified. The calibration procedure includes (i) the correction of isotope measurements at low

https://doi.org/10.5194/tc-2020-302
Preprint. Discussion started: 27 October 2020


The Cryosphere Discussions

humidity by determining the required humidity-response functions of the Picarro analyser, (ii) corrections of a potential long-term drift of the instrument, (iii) the correction for an offset between measured and real isotope values, and (iv) filtering the data of special events, -e.g. weather conditions with a potential contamination of our vapour measurements by the station's exhaust gases, or days with temperature stabilization problems in the cooler boxes.

The range of humidity defined for the Picarro analyser is 1000 to 50000 ppm. At Neumayer Station, relative humidity easily reaches values below 1000 ppm in the austral winter. For humidity values lower than 2000 ppm, the analyser shows systematic errors with biases of more than 1 ‰ for $\delta^{18}O$ (Casado et al., 2016). To correct these systematic errors, we need to assess humidity-response functions for our Picarro analyser. Humidity-response functions for all four isotope standards are determined once every year. Isotope values for absolute humidity ranging between 100ppm and 10000ppm are measured several times and a best-fitting curve (2^{nd} degree polynomial) is calculated. We do not find any change in the fitting curve between the different years of calibration. For determining and correcting an instrumental drift and offset, all isotope standards are measured every 25 hours. The measured isotope values are compared to the expected real standard isotope values for offset correction and measured isotope values over a period of 14 days are considered for drift correction. Screening of the data for special events with anomalous vapour or isotope data are performed afterwards.

During the calibration procedure, water vapour is produced from the liquid isotope standard within the bubbler system. Over the course of a year, this might lead to a change in the isotopic composition of the liquid standards. To correct for a potential change in the standards, samples from all liquid standards are taken and measured yearly.

The uncertainty of measurements contains the accuracy and the precision on corrected measurements using error propagation method. The accuracy is calculated based on a calibration program, considering the instrumental drift, deviation from known isotopic values, and systematic error according to humidity response functions and the precision is based on taking average on measured data for 1-hour corrected data as the output of the calibration program. From the determined humidity-response functions and calibration procedure, we estimate the mean uncertainty of the Picarro isotope data over the whole observational period as 0.45 ‰ for $\delta^{18}O$, 2.99 ‰ for δD, and 3.03 ‰ for d–excess values.

2.4 Moisture source diagnostics

To study the origin and transport paths of water vapour to Neumayer Station, the Lagrangian particle dispersion model FLEXPART (Brioude et al., 2013) enhanced by a Lagrangian moisture source diagnostic (Sodemann et al., 2008) is used in this study. Meteorological data needed for the FLEXPART model are taken from the ERA-Interim reanalysis dataset (Dee et al., 2011), provided by the European Centre for Medium-Range Weather Forecasts (ECMWF). Due to computational constraints, we restricted our FLEXPART analyses to the year 2017, only. Air parcels are traced backwards from the final destination (Neumayer Station) for 10 days, similar to the setup described by Sodemann et al. (2008). The moisture source diagnostic based on the Lagrangian back-trajectories provides values of "moisture uptake" (in $mm\ day^{-1}$) on a $1^\circ \times 1^\circ$ grid. This parameter represents the amount of moisture injected to the air masses within each grid cell, contributing to the humidity at Neumayer Station.

https://doi.org/10.5194/tc-2020-302
Preprint. Discussion started: 27 October 2020


The Cryosphere Discussions

3 Results

3.1 Temperature and water vapour measurements

For the observational period 17 February 2017 until 22 January 2019, daily mean values of temperature, humidity, $\delta^{18}O$, δD, and d–excess have been determined (Fig. 2). There exist some data gaps for humidity and related isotope values for these two years of measurements. Water vapour isotope data is missing at some days because of maintenance or reparation of the instrument, measuring humidity response functions, or due to the removal of data outliers related to instable measurements of the Picarro instrument. In total, daily vapour and isotope data exists for 600 out of 705 days (85 %).

Daily temperatures at Neumayer Station vary between approximately 0°C in austral summer and -40°C in austral winter. Daily values of humidity vary between 0.06 $g\ kg^{-1}$ (corresponding to approx. 100 ppm) and 3.75 $g\ kg^{-1}$ (approx. 6000 ppm). Daily mean $\delta^{18}O$ (δD) values of the vapour vary in a range between -48.79 ‰ and -18.10 ‰ (-380.07 ‰ and -141.67 ‰). For the d–excess, the values range approximately from -5 ‰ to +35 ‰. The annual mean values of all variables except d–excess do not show a significant change (the change is less than the mean uncertainty for hourly data) between the first and second year of measurements. The average 2 m temperature for the year 2017 and 2018 is -15.81°C and -15.65°C, respectively. Both values are close to the long-term annual temperature of -15.97°C (mean of the years 1981 to 2018). For $\delta^{18}O$ (δD), the mean annual values for the first and second year of measurements are -33.30 ‰ and -33.08 ‰ (-253.35 ‰ and -255.17 ‰), respectively. For d–excess, mean annual values for the first and second year are 13.06 ‰ and 9.50 ‰. The annual average of humidity for 2017 and 2018 is 1.18 $g\ kg^{-1}$ and 1.23 $g\ kg^{-1}$.

Temperature, humidity, $\delta^{18}O$, and δD show a clear seasonal cycle in the daily mean data series (Fig. 2) with high values at the end of austral summer (January–February) and low values at the end of austral winter (August–September). No such seasonal cycle is observed for the d–excess. While d–excess values are constantly decreasing between February 2017 and February 2018, small variations with a peak in autumn 2018 can be detected until January 2019. Due to the limited period of two years, the dataset is too short to determine if any seasonal cycle of d–excess exists in our measurements. This is even more true, as the uncertainty of the measured isotope values depends on the humidity amount, which is much lower at Neumayer Station in austral winter as compared to the summer season. Based on the determined mean uncertainty of the 1-hour Picarro data (Chapter 2), we estimate the monthly average uncertainty for d–excess in austral winter as high as 4.5 ‰ (for July 2017) while it decreases during austral summer down to 1.9 ‰ (for November 2017, see Table 2).

For evaluation and calibration of the vapour data measured with the Picarro analyser, we compare the measured humidity values measured with humidity values measured at the meteorological station of Neumayer Station (Schmithüsen et al., 2019). These measurements are performed in a distance of 50 meters from the main station building at a height of 2 meters. A comparison of both datasets indicates that the Picarro analyser data are reliable (Fig. 3). The correlation coefficient between these two totally independent humidity measurements is 0.97 ($N = 12198$, hourly values between 17 February 2017 and 22 January 2019). The relationship between these two series of humidity measurements ($q_{Picarro} = 1.5 q_{meteorology} + 0.08$, standard error of the estimate = 0.0022 $g\ kg^{-1}$) has been used for the calibration of the humidity values measured by the Picarro analyser.

https://doi.org/10.5194/tc-2020-302
Preprint. Discussion started: 27 October 2020

The Cryosphere Discussions
Open Access
EGU

Table 1. The monthly mean values and uncertainty (calculated from hourly data) for $\delta^{18}O$, δD, and d–excess from February 2017 to January 2019.

	$\delta^{18}O$ ‰		δD ‰		**d–excess ‰**	
Month	mean	uncertainty	mean	uncertainty	mean	uncertainty
2017-2	-27.98	0.32	-205.33	2.45	18.52	2.48
2017-3	-33.30	0.50	-244.85	3.57	21.54	3.61
2017-4	-31.66	0.33	-231.04	2.35	22.21	2.38
2017-5	-36.78	0.51	-277.82	3.33	16.43	3.40
2017-6	-39.03	0.66	-298.03	4.08	14.18	4.14
2017-7	-40.72	0.69	-311.68	4.43	14.08	4.49
2017-8	-39.56	0.51	-306.20	3.29	10.27	3.34
2017-9	-35.65	0.47	-273.79	3.13	11.40	3.17
2017-10	-32.10	0.27	-247.20	1.90	9.57	1.92
2017-11	-29.64	0.28	-227.72	1.86	9.40	1.88
2017-12	-26.88	0.33	-209.62	1.88	5.38	1.90
2018-1	-26.35	0.34	-207.00	1.98	3.77	2.00
2018-2	-29.94	0.57	-228.65	2.46	10.91	2.49
2018-3	-25.83	0.42	-200.33	2.48	6.30	2.51
2018-4	-33.04	0.58	-256.36	3.77	7.96	3.82
2018-5	-30.90	0.42	-239.45	2.71	7.77	2.74
2018-6	-36.94	0.58	-285.62	3.88	9.91	3.92
2018-7	-40.21	0.48	-312.19	2.87	9.50	2.91
2018-8	-41.14	0.64	-319.79	3.75	9.29	3.81
2018-9	-37.74	0.49	-290.86	3.08	11.09	3.12
2018-10	-37.73	0.56	-287.14	3.53	14.66	3.58
2018-11	-31.50	0.37	-240.29	2.50	11.73	2.53
2018-12	-27.34	0.52	-208.38	3.46	10.34	3.50
2019-1	-24.70	0.41	-193.01	2.47	4.56	2.50

https://doi.org/10.5194/tc-2020-302
Preprint. Discussion started: 27 October 2020

The Cryosphere Discussions
Open Access
EGU

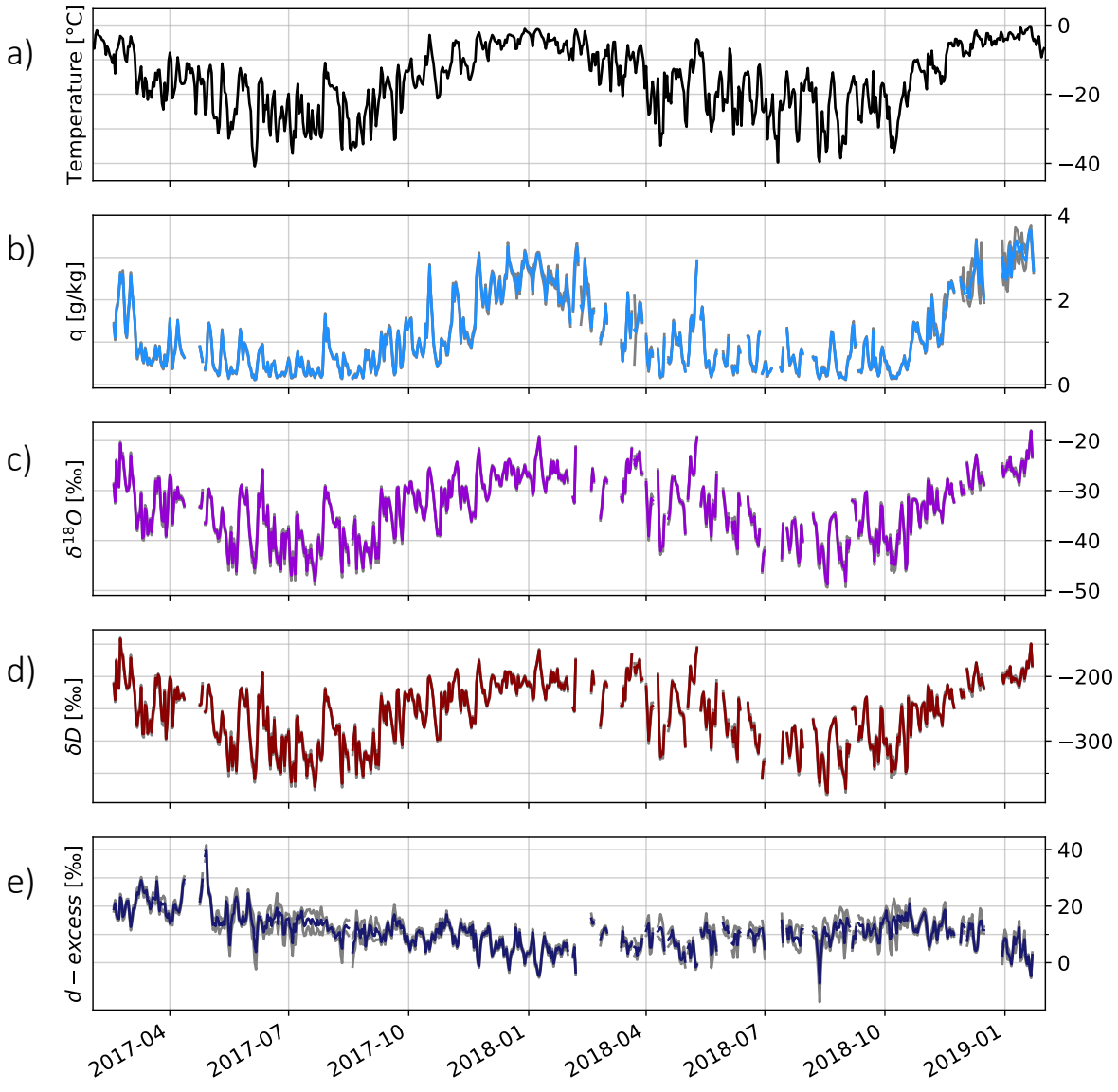

Figure 2. Daily averaged observations at Neumayer Station from February 2017 to January 2019. Downward: a) 2 m temperature [°C]; b) specific humidity [$g\ kg^{-1}$]; c) $\delta^{18}O$ [‰]; d) δD [‰]; e) d–excess [‰]. The determined uncertainties of the Picarro instrumental data (see text) are plotted as gray lines.

Our comparison yields a relatively high number of the Picarro analyser hourly humidity values, which are much higher than the fitted line (Fig. 3). These high humidity values could stem from height differences between the Picarro analyser and the meteorological sensor. A humidity inversion might have existed at the time of those vapour measurements, with lower

https://doi.org/10.5194/tc-2020-302
Preprint. Discussion started: 27 October 2020

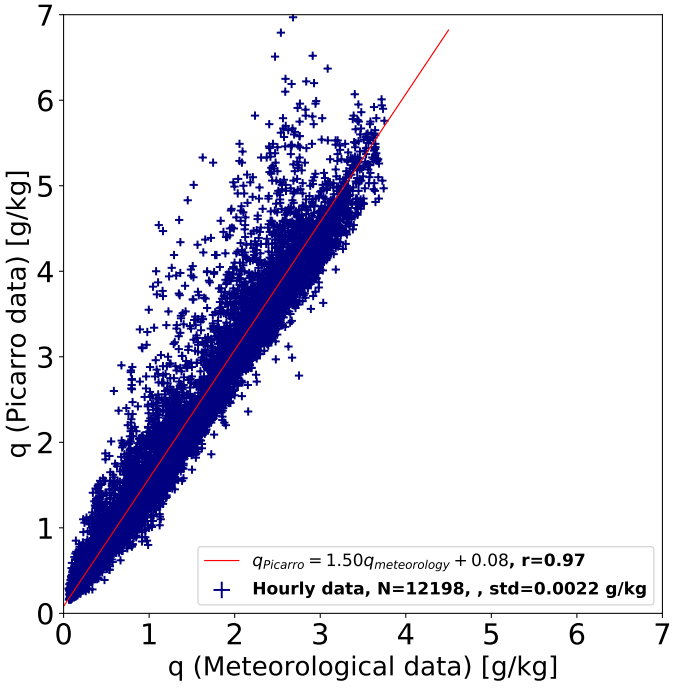

Figure 3. Hourly averaged humidity values measured by a meteorological sensor vs. humidity values measured by the Picarro instrument at Neumayer Station from February 2017 to January 2019. Humidity values are given in $g\ kg^{-1}$.

humidities close to the surface due to hoar frost formation, which locally removes moisture from the atmosphere. The inlet of the Picarro instrument is situated approximately 17.5 m above the surface level of the station. As the station is placed on a small artificial hill, this surface level is approx. 7.6 m higher than the surface level of the meteorological mast placed 50m besides the station building. Thus the total height difference between the Picarro inlet and the height of the meteorological humidity measurements is approximately 22 m. To test if contamination by exhaust gases could be another reason for this data mismatch, the wind direction was analysed for those hourly Picarro humidity values which are much higher than the corresponding humidity values measured by the meteorological station. Most of the outliers coincide with a wind direction from the south (and a few from the east), which excludes the possibility that a contamination by exhaust gases is the reason for the unusually high Picarro humidity values.

3.2 Relationships between water vapour isotopes and local climate variables

Next, we analyse the relationship between $\delta^{18}O$, δD, temperature and humidity to determine the key meteorological variables controlling the isotope signals in vapour at Neumayer Station.

https://doi.org/10.5194/tc-2020-302
Preprint. Discussion started: 27 October 2020

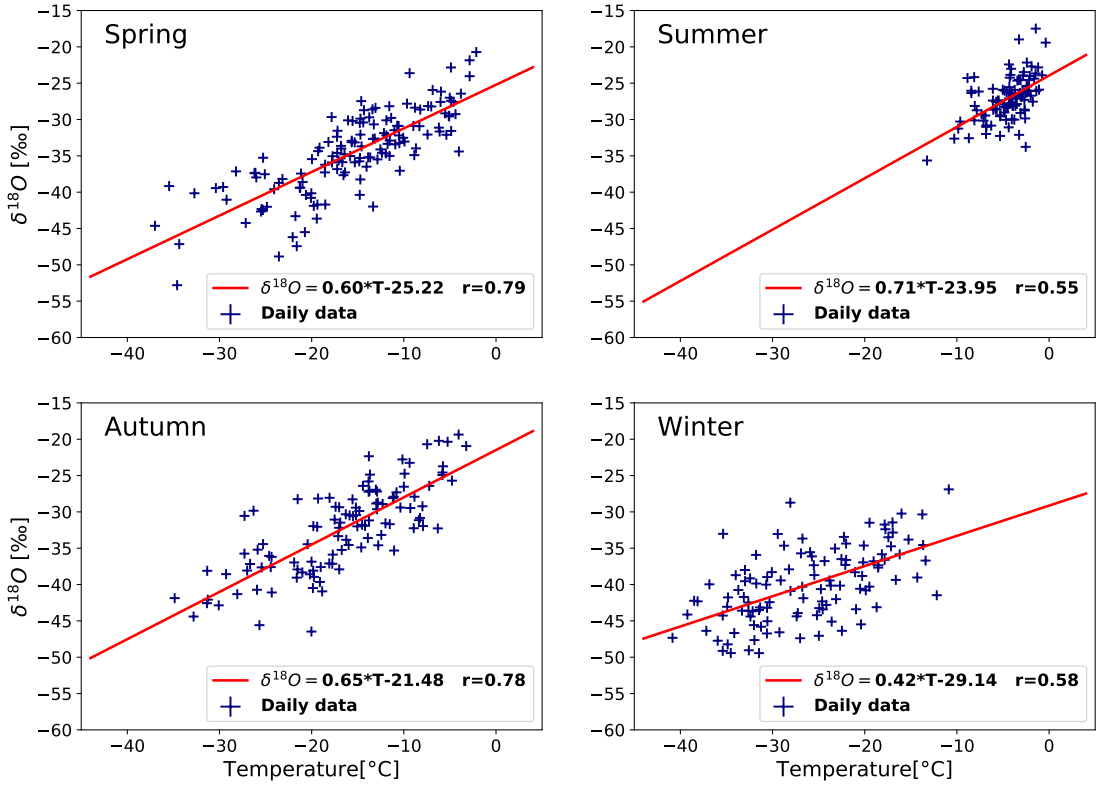

Figure 4. $\delta^{18}O$ [‰] vs. temperature [°C]. Four plots show daily average temperature–$\delta^{18}O$ values for different seasons of the year. For each season, a best fitted line, using the least-squares approach, for $\delta^{18}O$ vs. temperature is plotted as a red line and corresponding correlation coefficients are calculated.

3.2.1 $\delta^{18}O$ vs. temperature

As expected for a high-latitude location, $\delta^{18}O$ (and also δD) is strongly correlated with the 2 m temperature. For daily averaged values, the relationship between 2 m temperature and $\delta^{18}O$ in water vapour is $\delta^{18}O = 0.58T - 24.01$ ($r = 0.89$).

Next, we look at different seasons of the year and evaluate the slope and correlation coefficient of the $\delta^{18}O - T_{2m}$-relationship for each season, considering daily average values. The slopes for spring, summer, autumn, and winter are 0.60 ± 0.04 ‰ $°C^{-1}$ ($r = 0.79$), 0.71 ± 0.11 ‰ $°C^{-1}$ ($r = 0.55$), 0.65 ± 0.05 ‰ $°C^{-1}$ ($r = 0.78$), and 0.42 ± 0.06 ‰ $°C^{-1}$ ($r = 0.58$), respectively. The temperature–$\delta^{18}O$ slope is highest for summer and lowest for the winter season (Fig. 4).

Daily temperature and $\delta^{18}O$ values in summer are less fluctuating than in the other three seasons (Fig. 4). This might be explained by the local meteorological conditions: the Neumayer Station is located on a 200 m thick ice-shelf always covered

https://doi.org/10.5194/tc-2020-302
Preprint. Discussion started: 27 October 2020

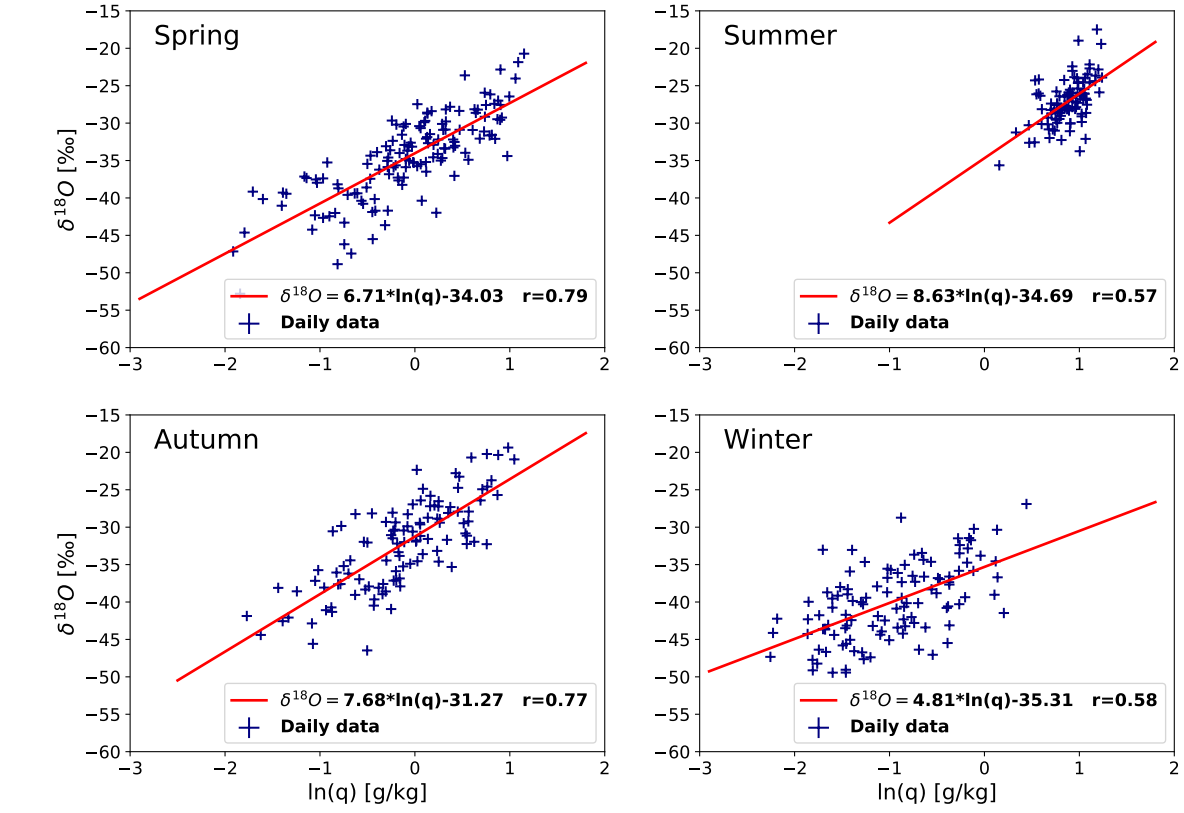

Figure 5. As Fig. 4, but for $\delta^{18}O$ [‰] vs. natural logarithmic humidity (ln(q)) [$g\ kg^{-1}$].

with snow. In summertime, when the air temperature can rise above $0°C$, the surface snow will reach its melting point and start to melt. For the melting process, the incoming radiative energy is partly used for latent heat uptake, keeping the near-surface temperature close to the melting point. Thus, even though the atmosphere temperature might go above zero, the surface and 2 m temperature will stay almost constant close to 0°C. This phenomena can explain the detected cutoff at 0°C of the 2 m temperature (Fig. 4) and might also partly explain the lower correlation coefficient between the 2 m temperature and $\delta^{18}O$ in summer, as the latter is most likely controlled by upper air temperatures.

3.2.2 $\delta^{18}O$ vs. humidity

The $\delta^{18}O$ (and δD) values of water vapour at Neumayer Station are strongly correlated to the natural logarithm of specific humidity, too ($r = 0.88$ for daily $\delta^{18}O$ values; Fig. 5). The correlation for $\delta^{18}O$ and ln(q) also varies in different seasons

https://doi.org/10.5194/tc-2020-302
Preprint. Discussion started: 27 October 2020

following the correlation coefficient between temperature and $\delta^{18}O$. To assess these variations quantitatively, we calculate the correlation coefficient of the natural logarithmic specific humidity and $\delta^{18}O$ for each season (based on daily data). The highest correlation coefficient is found in spring $r = 0.79$) and the lowest one in summer ($r = 0.57$). Like the summer temperature values, the summer humidity values at Neumayer appear to be limited, with a maximum value of approx. 4 $g\ kg^{-1}$ (Fig. 5). The reason might be the same as for the observed temperature limit.

3.2.3 $\delta^{18}O$ vs. δD and d–excess

Daily values of $\delta^{18}O$ and δD reveal a high correlation coefficient ($r = 0.99$), with a $\delta^{18}O$–δD slope of 7.67 ‰‰$^{-1}$ (Appendix, Fig. A1). For the Deuterium excess, an overall weak negative correlation between $\delta^{18}O$ and d–excess ($r = -0.35$) is found. For d–excess, the correlation with 2 m temperature is low and negative ($r = -0.25$). The corresponding correlation of the humidity with d–excess is slightly stronger ($r = -0.40$).

Analysing different seasons of the year, a negative correlation between $\delta^{18}O$ and d–excess is detected for spring ($r = -0.47$), summer ($r = -0.51$), and autumn ($r = -0.37$), but for winter, no correlation exists (Appendix, Fig. A2). This pattern can be detected also for temperature-d–excess and humidity-d–excess relations (Appendix, Fig. B1 and B2). There is a negative correlation coefficient between temperature and d–excess for spring ($r = -0.28$), summer ($r = -0.38$), and autumn ($r = -0.19$), but in winter a weak positive correlation ($r = 0.17$) is noticed (Appendix, Fig. B1). Anti-correlations between the natural logarithmic humidity values and d–excess for spring (-0.29), summer (-0.43) and autumn ($r = -0.21$) are slightly stronger than the ones between temperature and d–excess. For winter, a weak positive correlation between natural logarithmic humidity values and d–excess ($r = 0.14$) is found (Appendix, Fig. B2).

3.3 Moisture source uptake and vapour transport

For further understanding of the seasonal different relations between $\delta^{18}O$, δD, Deuterium excess, and the meteorological variables, we analyse potential seasonal differences in the main moisture uptake areas for vapour transported to Neumayer Station, as simulated by FLEXPART (Fig. 6). In spring, major moisture uptake and transport happens from oceanic areas northwest of the station at high to mid-latitudes. In summer, most of the moisture uptake occurs in the coastal areas close to the station and in the South Atlantic Ocean, although in summer more humidity comes to the station. In autumn, moisture uptake occurs again mainly close to or east of the station, similar to summer. For winter, the moisture amount transported to the station is substantially less than in other seasons and comes from a wide area of the Southern Ocean, partly even from the Pacific.

3.4 Wind and pressure pattern

The origin of the air masses measured at Neumayer Station depends directly on the local wind, which is characterized by relatively high wind speeds, with an annual mean value of 8.7 $m\ s^{-1}$ (standard deviation= 6.1 $m\ s^{-1}$). Two main wind directions are found (Fig. 7). The prevailing wind direction is east, caused by the passage of cyclones north of the Antarctic

https://doi.org/10.5194/tc-2020-302
Preprint. Discussion started: 27 October 2020

The Cryosphere Discussions
Open Access
EGU

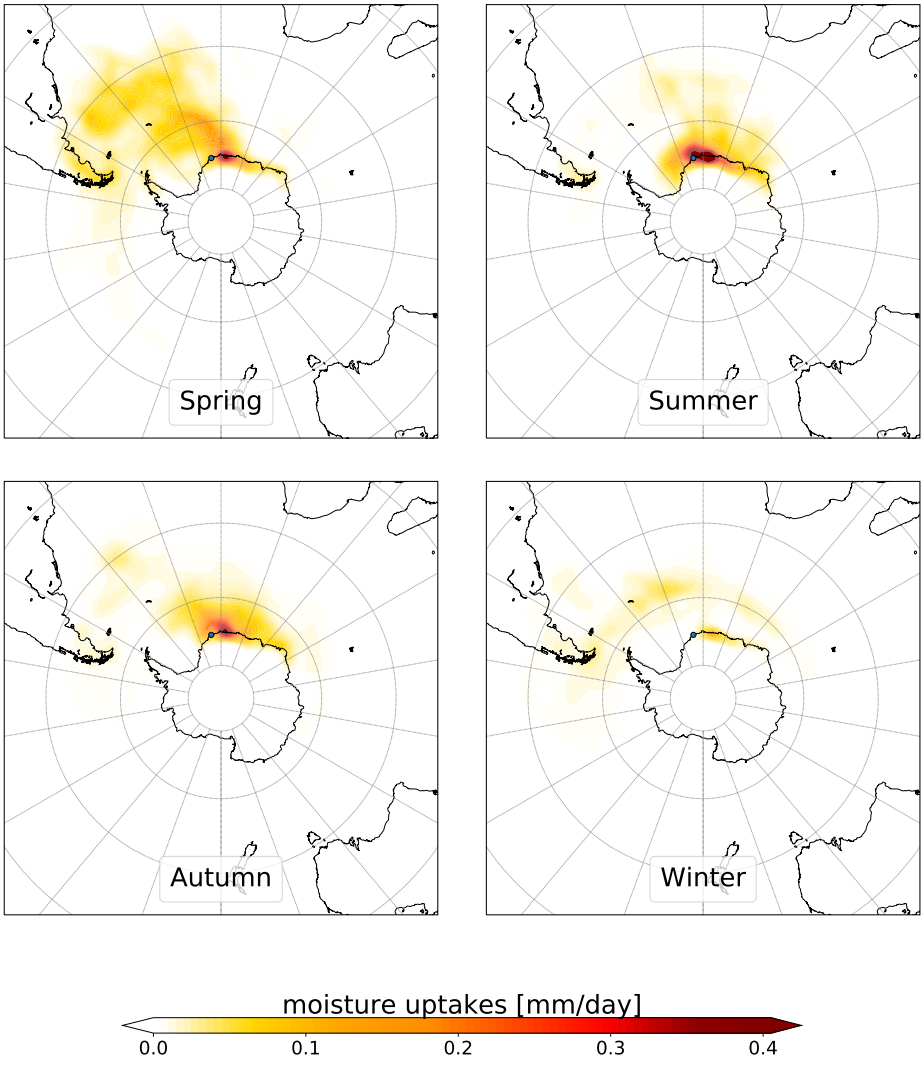

Figure 6. Simulated moisture uptake occurring within the boundary layer [$mm\ day^{-1}$] in the pathway to Neumayer Station during last 10 days modelled by FLEXPART using ECWMF, for spring (SON), summer (DJF), autumn (MMA), and winter (JJA).

coast in the circumpolar trough. For our observation period, the highest hourly wind speed value was 37.7 $m\ s^{-1}$ from the east.

The second, less frequent, typical wind direction is south to southwest, caused by a mixture of weak katabatic and synoptic influence, when Neumayer Station is situated between a cyclone to the east and an anticyclone to the west.

Pure katabatic winds are rare and restricted to extended high-pressure systems. Because the Ekström ice shelf slope is gently upward to the south, katabatic wind remains below 10 $m\ s^{-1}$ (south-north direction).

https://doi.org/10.5194/tc-2020-302
Preprint. Discussion started: 27 October 2020

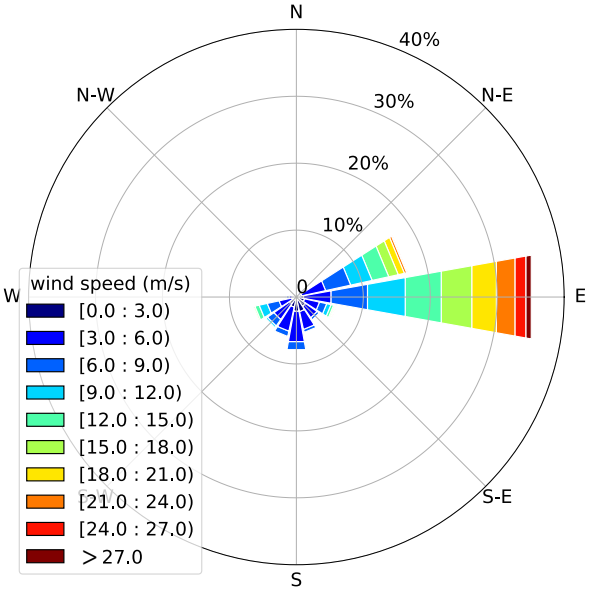

Figure 7. Two-dimensional frequency distribution of 10 m wind (measured every minute) at Neumayer Station in two years (February 2017–January 2019).

In addition to the local wind at Neumayer Station, vapour transport to the station is also strongly controlled by the larger-scale pressure and wind pattern. For all seasons, generally there is a high-pressure system above the Antarctic continent and a low-pressure belt surrounding the coast, thus north of the station (Fig. 8). This pressure pattern puts the station on average at the southern edge of a low-pressure system, which leads to a cyclonic circulation that transports vapour from the Southern Atlantic to Neumayer Station from easterly directions. As the pressure pattern related to this circulation is weakened in summer, far-field transport of vapour to Neumayer Station is reduced as compared to other seasons (Fig. 6).

4 Discussion

4.1 Key controls on vapour $\delta^{18}O$

4.1.1 Temperature and humidity

Relatively high correlations between daily $\delta^{18}O$ and temperature ($r = 0.89$), also between daily $\delta^{18}O$ and humidity ($r = 0.88$), highlight the role of temperature and humidity as the main drivers of $\delta^{18}O$ variations in water vapour. But how do these factors control $\delta^{18}O$ variations and how independent are they?

https://doi.org/10.5194/tc-2020-302
Preprint. Discussion started: 27 October 2020

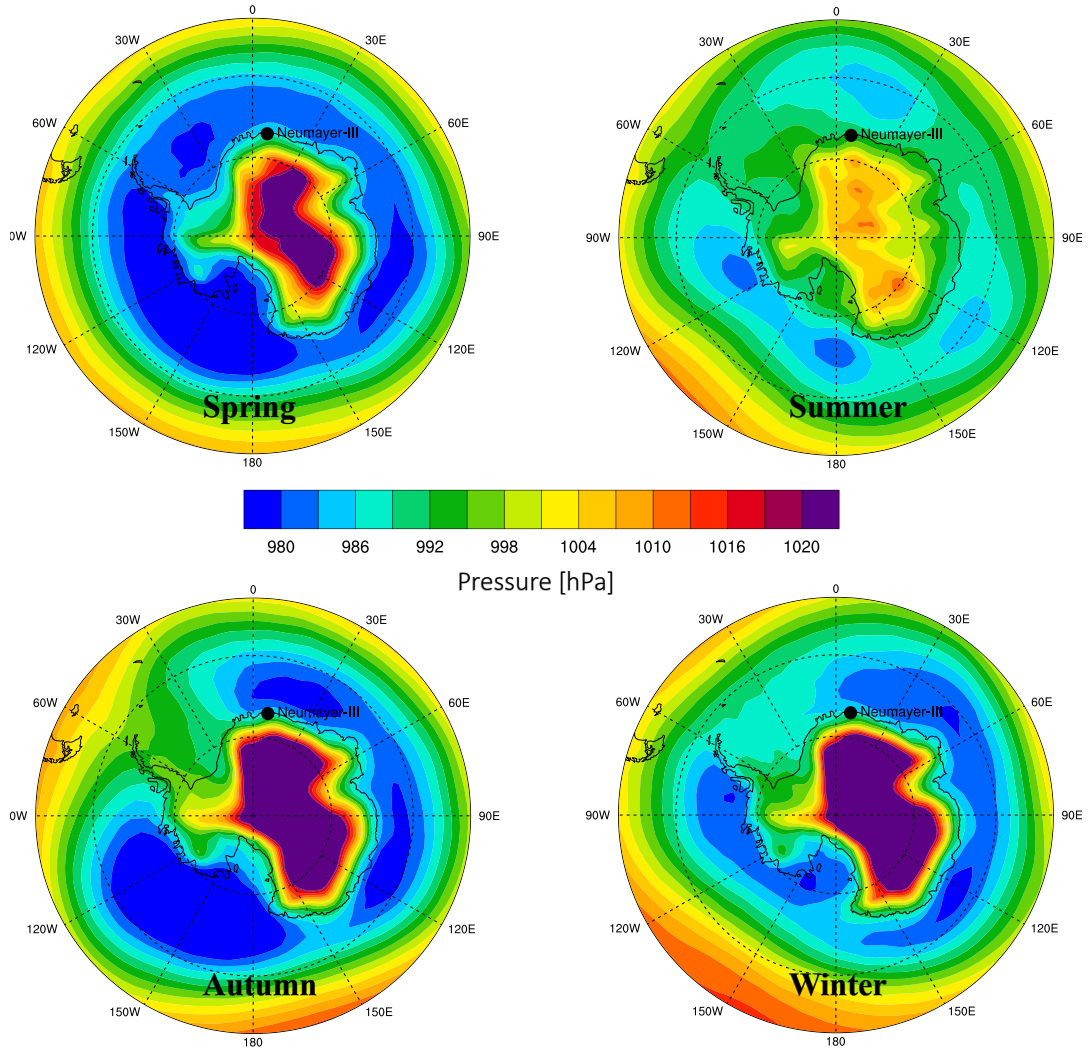

Figure 8. Seasonal (austral) mean sea level pressure. Meteorological data are taken from the ERA-Interim reanalysis dataset (Dee et al., 2011). Pressures are given in [hPa].

When the temperature around an air parcel decreases, water vapour condenses, which results in decreasing $\delta^{18}O$ value in water vapour and also decreasing humidity in the air parcel. Since Neumayer Station is a coastal station and the main air path is a cyclonic circulation that transports vapour from the ocean, the humidity and as a result $\delta^{18}O$ values, drop intensively in a distance between open sea and the station (16 km in northern direction), due to the temperature reduction over the shelf ice. This indicates that strong condensation happens in the areas close to the station that can explain the high correlation between local temperature and $\delta^{18}O$.

https://doi.org/10.5194/tc-2020-302
Preprint. Discussion started: 27 October 2020

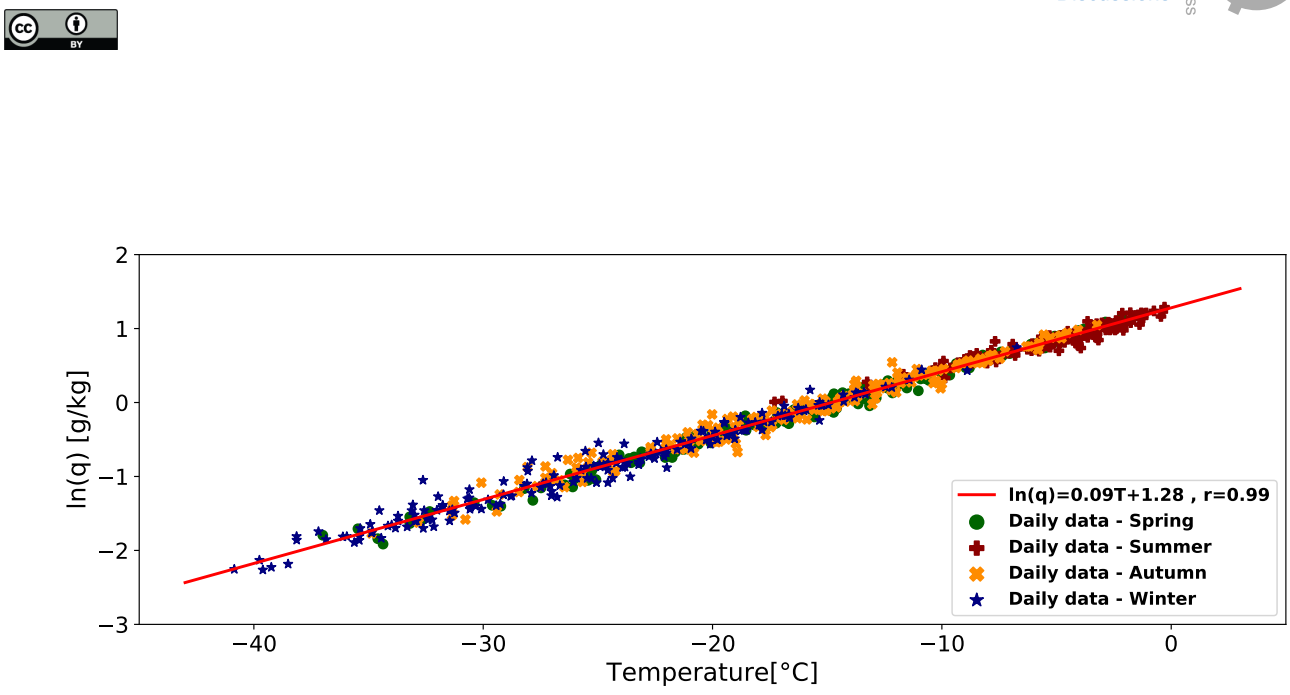

Figure 9. Temperature [°C] vs. natural logarithmic humidity [$g\ kg^{-1}$]. Daily average values for two years of experiment for different seasons (defined with different markers and colours) are shown. A best fitted line, using the least-squares approach is plotted as a red line and corresponding correlation coefficient is calculated.

Atmospheric temperatures and humidity values are closely linked via the Clausius-Clapeyron equation. We have checked this link for the Neumayer Station data, and find indeed a high correlation between temperature and natural logarithmic humidity values ($r = 0.99$; Fig. 9). Thus, the high correlation between humidity and $\delta^{18}O$ can be explained by the high correlation of temperature with both $\delta^{18}O$ and humidity. As isotopic fractionation is primarily controlled by temperature, we therefore estimate for the typical synoptic situation at Neumayer Station temperature fluctuations as the main driver for both changes in humidity and the $\delta^{18}O$ signal in water vapour.

4.1.2 Wind

Next we analyse the impact of another important climatic factor, wind, on the isotope values in vapour at Neumayer Station. In order to filter out the dominant temperature control on $\delta^{18}O$ in this analysis, we proceed as follows: we calculate a "predicted" daily $\delta^{18}O$ value in vapour, based on the corresponding daily temperature value and the observed relationship between temperature and $\delta^{18}O$ in vapour ($\delta^{18}O = 0.58T - 24.01$; see above). Then we look at the residual between the predicted $\delta^{18}O$ value and the observed $\delta^{18}O$ value (Fig. 10) and analyse how this residual might be linked to different wind pattern at Neumayer Station. First, we include in our analyses only days with no extreme high or low temperatures (as defined in Chapter 2.2). For this subset of days, we find that for 64 % of the days with the wind coming from the east and wind speed above the daily average easterly wind of 10.56 $m\ s^{-1}$ (22 out of 36 days), the measured $\delta^{18}O$ values are higher than the predicted $\delta^{18}O$ value. This indicates that even for days, when no strong temperature changes can be observed, strong winds from the east coincide with more enriched $\delta^{18}O$ values in water vapour at Neumayer Station. On the opposite, for 76 % of the days with katabatic

https://doi.org/10.5194/tc-2020-302
Preprint. Discussion started: 27 October 2020

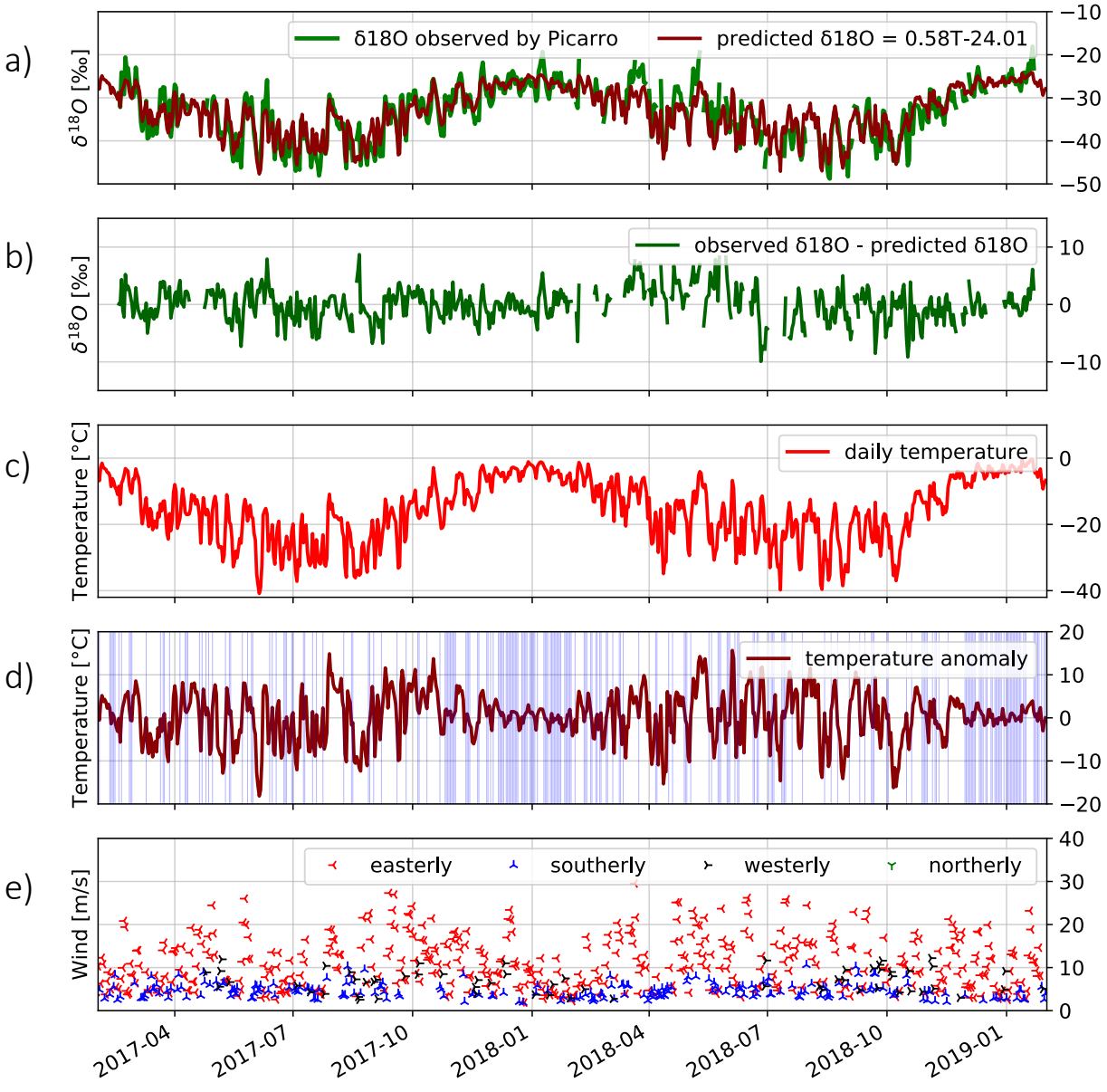

Figure 10. Daily observation time series at Neumayer Station from February 2017 to January 2019. Downward: a) green: observed $\delta^{18}O$, dark red: predicted $\delta^{18}O$ based on the annual relation between temperature and $\delta^{18}O$; b) observed $\delta^{18}O$ minus predicted $\delta^{18}O$; c) 2 m temperature [°C]; d) 2 m temperature minus multi-year daily temperature averages (from 1981 to 2018). Days with no temperature events are highlighted with blue colour; e) wind speed [$m\ s^{-1}$] and wind direction: red: easterly, blue: southerly, black: westerly, and green: northerly.

https://doi.org/10.5194/tc-2020-302
Preprint. Discussion started: 27 October 2020

The Cryosphere Discussions
Open Access
EGU

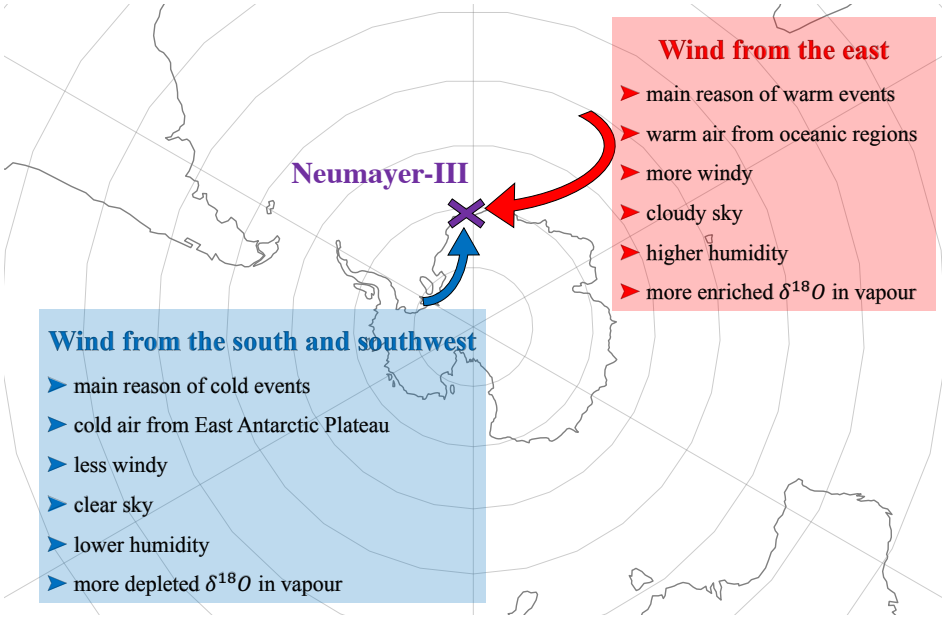

Figure 11. Frequent wind patterns (the first, easterly wind, and the second, southerly and south-westerly wind) at Neumayer Station and their characteristics.

winds and a wind speed higher than the daily averaged southerly wind of 4.56 $m\ s^{-1}$ (12 out of 17 days), measured $\delta^{18}O$ values are lower than the predicted $\delta^{18}O$ values. This means that southerly winds can transport water vapour with a more depleted $\delta^{18}O$ composition to the station, and such transport might occur without any significant temperature change.

Next, we analyse wind days with extreme high or low temperatures. During the observation period, on 86 % of all days with a warm temperature event at Neumayer Station, the wind came from the east. Such wind conditions are usually a result of a low-pressure system north of the station. In such a situation, the weather at Neumayer Station is typically relatively warm with high humidity (88% of days with a relative humidity higher than 90% coincide with wind from the east) and cloudiness (85% of cloudy days, means days with a total cloud amount more than 80%, coincide with this wind). In this wind pattern, relatively higher temperature and humidity leads to more enriched $\delta^{18}O$ values. During days with extreme low temperatures, the wind typically comes from south to southwest, and winds are generally weak. This weather pattern occurs when a cyclone has moved eastward, so that the former low-pressure area is replaced by a high-pressure ridge. In such a situation, wind speeds decrease and the wind direction changes from easterly to southerly and southwesterly. The weak katabatic winds are strengthened by the synoptically caused air flow and bring cold and dry air from the East Antarctic Plateau to Neumayer Station, usually dissolving the clouds. Lower temperature and humidity result in more depleted $\delta^{18}O$ in water vapour coming to Neumayer Station. Wind patterns and their effect are summarized in Fig. 11.

https://doi.org/10.5194/tc-2020-302
Preprint. Discussion started: 27 October 2020


The Cryosphere Discussions
Open Access
EGU

4.2 Key controls on vapour d–excess

Changes of d–excess in vapour generally are supposed to reflect different climate conditions at the moisture source region (Merlivat and Jouzel, 1979; Pfahl and Sodemann, 2014). For Neumayer Station, the Deuterium excess in vapour is weakly anti-correlated with the 2 m temperature ($r = -0.25$). The correlation between d–excess and humidity is slightly higher ($r = -0.40$), but not very strong neither. The analyses of the wind pattern revealed that there are two main pathways for air parcels transported to Neumayer Station, they stem either from the east or from the south-southwest. The main differences between these pathways are related to humidity (humid air from the ocean versus dry air from inland) and temperature (relatively warm air from the ocean versus cold air from inland). Using the back-trajectory analysis with the FLEXPART model, different areas of moisture uptaken, from locations close to the station to regions of the Southern Atlantic, could be identified.

In order to better understand the effect of different pathways and water moisture origins that control d–excess changes in vapour at the station, days with extreme values of d–excess are examined. The analysis is restricted to the year 2017 due to the above mentioned computational constraints related to the FLEXPART model simulation.

As no long-term measurements for d–excess in water vapour at Neumayer Station exist, we cannot define extreme d-excess values considering multi-year daily average (as done for the analysis of extreme temperature events). Thus, we define extreme d–excess values as daily averaged d–excess values which are one standard deviation higher or lower than the 10-days average value centered around the corresponding day (5 days before and 5 days after). Using this definition, 26 days with extreme high d–excess values and 37 days with extreme low d–excess values occur in the year 2017. In 70 % of the events, high d–excess values coincide with a daily humidity value lower than the corresponding 10-days humidity average value (5 days before and 5 days after the event). Similarly, for 63 % of the days with extreme low d–excess values, daily humidity values are higher than the corresponding 10-days humidity average. These findings suggest a significant link between extreme d–excess values in vapour and humidity itself. Looking at the temperature during days with extreme d–excess values shows that these events are relatively independent from extreme daily temperature values. For only 57 % of days with extreme low d–excess values and 58 % of days with extreme high d–excess values, daily temperature values are lower than the corresponding 10-days temperature average. Analysing the simulated moisture uptake for days with low and high d–excess values reveals the influence of the origin of the water vapour on extreme d–excess values (Fig. 12). The moisture corresponding to low daily d–excess values is either uptaken in coastal are as east of the station (this occurs mostly in summer) or northwest of it in the South Atlantic Ocean. The moisture corresponding to high daily d–excess values is mostly uptaken from locations close to the station. .

4.3 Reliability of back trajectory calculation

Wind direction and wind speed are two of the main factors used in our back trajectory calculations to determine the origin of air parcels heading to Neumayer Station. To check the robustness of our results, we compare ERA-Interim data wind data, which is used in this study for FLEXPART simulations to identify moisture sources and transport pathways to Neumayer Station, with meteorological observations from Neumayer Station. The comparison reveals that the ERA-Interim dataset reproduces wind direction and wind speed around Neumayer Station well for most days (Fig.13). However, for cold events, the ERA-Interim

https://doi.org/10.5194/tc-2020-302
Preprint. Discussion started: 27 October 2020

The Cryosphere Discussions
Open Access
EGU

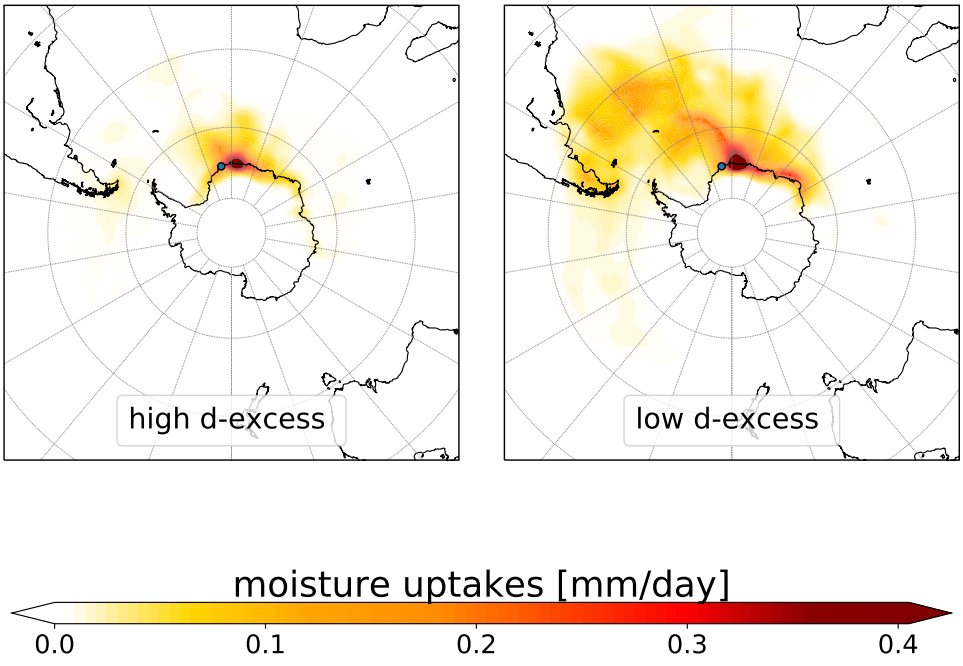

Figure 12. Simulated moisture uptake occurring within the boundary layer [$mm\ day^{-1}$] towards Neumayer Station modelled by FLEXPART, left: an average on days with high d–excess events, right: an average on days with low d–excess events.

dataset has a bias with respect to the observed frequency of southerly winds. The main reason for this bias in the ERA-Interim data might be the low number of stations in Antarctica, which are used to generate the ERA-interim reanalysis dataset. Due to this bias in the ERA-Interim data, the simulated moisture uptake and vapour transport pathways during cold events, when katabatic winds from the south occur at Neumayer Station, should be taken with caution.

4.4 Comparison of water stable isotope measurements in Antarctic vapour

To further assess the results of our water stable isotopes measurements in vapour at Neumayer Station, we look at comparable vapour measurements in Antarctica. To our knowledge, our study is the first one measuring water isotopes in vapour in Antarctica throughout the whole year. Other studies have been performed only during austral summer (mostly December and January), for limited periods of 40 days or less (Ritter et al., 2016; Casado et al., 2016; Bréant et al., 2019). Thus, for the comparison of our data with these previous studies, we focus on our austral summers results (December 2017/January 2018 and December 21018/January 2019), only.

https://doi.org/10.5194/tc-2020-302
Preprint. Discussion started: 27 October 2020

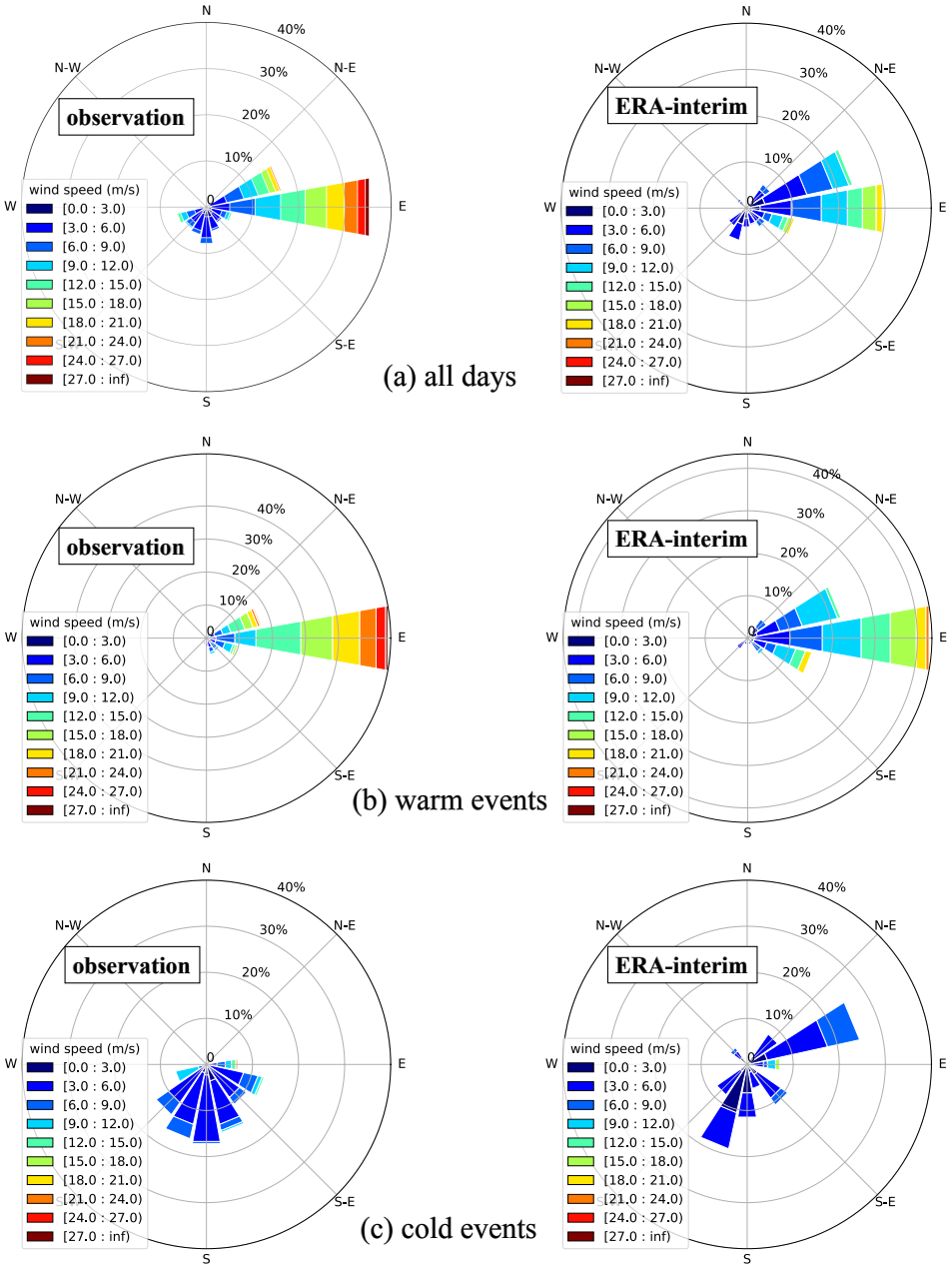

Figure 13. Two-dimensional frequency daily 10 m wind (stated in $m\ s^{-1}$) at Neumayer Station during the year of 2017 provided by observations and ECMWF (ERA-Interim) data for (a) all days of the year, (b) days considered as warm events, (c) days considered as cold events.

https://doi.org/10.5194/tc-2020-302
Preprint. Discussion started: 27 October 2020

4.4.1 Dumont d'Urville station in Adélie Land

Most comparable to our measurements is a recent study by Bréant et al. (2019), who have reported water isotopes in vapour from the Dumont d'Urville station in Adélie Land, which is also located at the Antarctic coast, however opposite to the Neumayer Station (Fig. 1). The average temperature at the Dumont d'Urville station during the study period was -0.5°C and the average value of $\delta^{18}O$ in vapour was -30.37 ‰. At Neumayer Station, $\delta^{18}O$ values in vapour related to a comparable summer temperature (-0.5 ± 0.05°C) are substantially more enriched (-24.47 ± 2.34 ‰). The lower $\delta^{18}O$ values at the Dumont d'Urville station can be explained by the prevailing katabatic winds at this location, which bring dry, depleted air from the continent to the Dumont d'Urville station. For the relationship between $\delta^{18}O$ and temperature, the correlation coefficient for Dumont d'Urville is $r = 0.49$ for clear-sky conditions and $r = 0.33$ for cloudy-sky conditions. Our all-sky summer value at Neumayer Station is $r = 0.55$. For better comparison with Dumont d'Urville station, we also calculated different values for cloudy and clear-sky conditions at Neumayer Station. To determine days with cloudy or clear sky at Neumayer Station, we used the same method as in Bréant et al. (2019). To do this, all days with the median long wave downward radiation values higher (lower) than 280 $W.m^{-2}$ are considered as days with a cloudy-sky (clear-sky). Our study shows a slightly higher correlation coefficient than at Dumont d'Urville station for both conditions at Neumayer Station (clear-sky: $r = 0.62$, cloudy-sky: $r = 0.53$). Bréant et al. (2019) argue that temperature cannot be a main driver for $\delta^{18}O$ in water vapour due to this low correlation coefficient, even for the clear-sky conditions. However, the correlation coefficient between $\delta^{18}O$ in vapour and humidity is high ($r = 0.85$) at Dumont d'Urville, but only for clear-sky conditions. When the sky is cloudy, quantities seem to be totally uncorrelated ($r < 0.01$). For Neumayer Station, this correlation exists for both conditions similarly, but lower than the one at Dumont d'Urville in clear-sky conditions (at Neumayer Station; for clear-sky: $r = 0.59$, for cloudy-sky: $r = 0.67$). At the Dumont d'Urville station, the correlation between d–excess and humidity in vapour is $r = -0.71$ for clear-sky conditions, while they are uncorrelated ($r < 0.01$) for cloudy-sky conditions. At Neumayer Station, d–excess and humidity in vapour are anti-correlated under cloudy-sky conditions ($r = -0.55$), but they are uncorrelated for clear-sky conditions ($r = 0.10$). At both stations, cold and dry air parcels from the continent, which are transported by katabatic winds to the stations, are characterized by low humidity, low $\delta^{18}O$, and high d–excess values. At Dumont d'Urville station, katabatic winds are the prevailing wind system due to its complex topography. They are on average considerably stronger than the katabatic winds observed at Neumayer Station and often lead to clear-sky conditions. In these situations, the amount of moisture transported by the katabatic winds to Dumont d'Urville station determines the $\delta^{18}O$ values in vapour. However, for Neumayer Station, the prevailing wind system is easterly winds bringing humid air with relatively high $\delta^{18}O$ values from the Southern Ocean to the station. But for days with katabatic winds at Neumayer Station, the effect of these cold, dry winds on the water stable isotopes composition in vapour appears to be qualitatively comparable to the situation at Dumont d'Urville station.

4.4.2 Kohnen Station, Dronning Maud Land

The location closest to Neumayer Station, at which vapour isotope measurements have been performed, yet, is the Kohnen station in Dronning Maud Land, with a distance of 757 km inland, SSE to Neumayer Station (Fig. 1). Kohnen Station is located

https://doi.org/10.5194/tc-2020-302
Preprint. Discussion started: 27 October 2020

Table 2. Comparison of summer water vapour isotope studies in different Antarctic stations (Ritter et al., 2016; Bréant et al., 2019). The time period of each study is shown in the table. For Neumayer Station, two months of two summers (December 2017/January 2018 and December 21018/January 2019) are considered.

	Neumayer	**Dumont d'Urville**	**Kohnen**
Location	coastal	coastal	inland
period of measurements	01/12/2017 - 31/01/2018 and 01/12/2018 - 19/01/2019	26/12/2016 - 03/02/2017	17/12/2013 - 21/01/2014
$\delta^{18}O$ **vs. temperature**	$r_{clear} = 0.62$ $r_{cloudy} = 0.53$ $r_{total} = 0.61$	$r_{clear} = 0.49$ $r_{cloudy} = 0.33$	$r = 0.49$
$\delta^{18}O$ **vs. humidity**	$r_{clear} = 0.59$ $r_{cloudy} = 0.67$ $r_{total} = 0.63$	$r_{clear} = 0.85$ $r_{cloudy} \approx 0$	$r = 0.56$
d–excess vs. humidity	$r_{clear} = 0.10$ $r_{cloudy} = -0.55$ $r_{total} = -0.26$	$r_{clear} = -0.71$ $r_{cloudy} \approx 0$	-no data-
$\delta^{18}O$ **vs.** δD	$r = 0.98$, $s = 6.7\,‰\,‰^{-1}$	-no data-	$r = 0.97$ $s = 6.2\,‰\,‰^{-1}$
main weather pattern	easterly wind	katabatic wind	katabatic wind

in a continental area of Antarctica at an elevation of 2892 m (Ritter et al., 2016). Water vapour isotopes were measured at this station for one month during the austral summer season 2013–2014 (Ritter et al., 2016). The mean temperature during the study period at Kohnen Station was -23.40°C which is approximately 20°C lower than the temperature at Neumayer Station during the same period. In accordance with this lower mean temperature, the water vapour at Kohnen Station was characterized by a lower mean $\delta^{18}O$ signal (-54.74 ‰) than the one at Neumayer Station (-39.11 ± 4.08 ‰ for considered temperature, -23.40°C). At Kohnen Station $\delta^{18}O$ is correlated with humidity ($r = 0.56$) and with temperature ($r = 0.49$). These correlation coefficients at Neumayer Station (for temperature–$\delta^{18}O$, $r = 0.61$, and for humidity–$\delta^{18}O$, $r = 0.63$, are higher than the respective values found at Kohnen Station during the 1 month measuring period, though. At both Neumayer Station and Kohnen Station, $\delta^{18}O$ and δD are also highly correlated ($r = 0.98$ and $r = 0.97$, respectively), but the slope between these variables at Neumayer Station is larger than the slope at Kohnen Station. Neumayer Station is a coastal station while Kohnen Station is a continental station. Although the two stations are relatively close to each other, they have very different climate conditions. At Kohnen Station, strong katabatic winds dominate the changes in isotopic values of water vapour, while at Neumayer Station winds from the east related to cyclonic weather pattern centered over the Southern Ocean play a major role (Medley et al., 2018).

The differences of the available summer data sets from these three locations (Neumayer Station, Dumont d'Urville, Kohnen Station) are summarized in Table 2.

4.5 Air-snow interaction

Recently, several studies have reported an exchange of water isotopes between surface snow and the vapour above the surface for Greenland (Steen-Larsen et al., 2014; Madsen et al., 2019) and Antarctica (Casado et al., 2018). Such exchange might be

https://doi.org/10.5194/tc-2020-302
Preprint. Discussion started: 27 October 2020

of high importance for an improved interpretation of past isotope variations measured in polar ice cores. Therefore, we also compare our vapour measurements to isotope measurements of snow in the vicinity of Neumayer Station. At Neumayer Station, fresh snow has been sampled after major snowfall events since 1981. In contrast to locations in the interior of Antarctica, snowfall events in coastal areas of the Ekström Ice Shelf, where the station is located, are evenly distributed over the whole year (Helsen et al., 2005). Mean isotope values of these snow samples from Neumayer Station are -20.54 ‰ for $\delta^{18}O$ and 153.25 ‰ for δD, for the period 1981 to 2000 (Schlosser et al., 2004). The slope between the 2 m temperature and $\delta^{18}O$ in the snow samples was determined as 0.57 ‰ $^{\circ}C^{-1}$ ($r = 0.69$) for the period 1981 to 2000 (Schlosser et al., 2004). This value was confirmed by Fernandoy et al. (2010), who found an identical T–$\delta^{18}O$ slope for snow samples of the extended period from 1981 to 2006. This reported slope in snow samples is very close to our findings for the relation between $\delta^{18}O$ in water vapour and the 2 m temperature (0.58 ‰ $^{\circ}C^{-1}$, $r = 0.87$). Additionally, we find a similar slope between $\delta^{18}O$ and δD in our vapour measurements (7.67 ‰ ‰$^{-1}$) for the period February 2017 to January 2019, as it has been reported for snow samples (7.95 ‰ ‰$^{-1}$) for the period 1981 to 2006 (Fernandoy et al., 2010). Schlosser et al. (2004) found that the T–$\delta^{18}O$ slope for the snow samples at Neumayer Station varies between 0.43 ‰ $^{\circ}C^{-1}$ and 0.75 ‰ $^{\circ}C^{-1}$, depending on the origin of the moisture and the transport path. By performing a back-trajectory analysis, the authors showed that a lower T–$\delta^{18}O$ slope in the snow samples corresponds to air parcels with an origin over the ocean, while higher T–$\delta^{18}O$ slopes are related to air parcels originating from continental areas. We consider in our vapour isotope measurements the data for only two years (February 2017 to January 2019) and calculate T–$\delta^{18}O$ slopes for different seasons of the year. The slopes range from 0.42 ‰ $^{\circ}C^{-1}$ to 0.71 ‰ $^{\circ}C^{-1}$, with the lowest slope occurring in austral winter for air parcels with a oceanic origin in lower latitudes. Higher slopes are found in austral summer, and our FLEXPART analyses reveal that the summerly water vapour originates in nearby coastal areas (the oceanic and continental areas close to the station).

Steen-Larsen et al. (2014) shows in their case study in Greenland, that surface snow $\delta^{18}O$ between snowfalls events, follows $\delta^{18}O$ in water vapour with similar or smaller changes than the water vapour $\delta^{18}O$. The authors suspect that surface snow isotopes are driven by changes in the water vapour isotopic compositions. In our study, the agreement in the T–$\delta^{18}O$ slopes and also in the $\delta^{18}O$–δD slopes for water vapour and snow samples measured at Neumayer Station is remarkable. Thus, the isotopic exchange between water vapour and surface snow at this location should be further examined in more detail in future research studies. If surface snow isotopic compositions are derived by changes in water vapour isotopes, ice core water isotope records might be interpreted as continuously recorded paleoclimate signals, even for periods without any precipitation.

5 Conclusions

In this study we analyse the first continuous measurements of water vapour isotopic composition at Neumayer Station, Antarctica, over a period of two entire years (February 2017 to January 2019). This unique data set makes it feasible to study not only summer conditions, but seasonal differences and variations of water vapour isotopes at an Antarctic station. Our measurements reveal a clear seasonal cycle of $\delta^{18}O$ and δD variations in vapour, with maxima at the end of austral summer and minima in austral winter. The variability of $\delta^{18}O$ and δD is hereby strongly driven by changes in local temperature and humidity, both

https://doi.org/10.5194/tc-2020-302
Preprint. Discussion started: 27 October 2020

on seasonal and shorter time scales. Generally, a stronger isotopic depletion in vapour at Neumayer Station can be associated with colder, dryer air from the south, whereas the vapour is isotopically enriched, when relatively warm easterly winds prevail. However, our data set does not clearly reveal a seasonal cycle for the Deuterium excess in vapour. This may be due to the low accuracy of the measurements in winter, when the humidity at Neumayer Station is extremely low. Despite this measurement uncertainty, d–excess shows a slightly stronger correlation with humidity than with temperature.

Similar findings as for Neumayer Station have been reported for Dumont d'Urville and Kohnen Stations, where also humidity was better correlated with $\delta^{18}O$ than temperature, however, for completely different reasons than at Neumayer Station. Whereas Dumont d'Urville is strongly influenced by katabatic winds, which advect cold and isotopically depleted air from the continent to the base, Kohnen Station is situated on the East Antarctic plateau in a dry and cold climate very different from conditions at Neumayer Station.

A comparison of vapour and snow isotope data shows that the slopes of both the temperature–$\delta^{18}O$ relationship and the $\delta^{18}O$–δD relationship is remarkably similar for snow and vapour at Neumayer Station. This similarity supports recent findings that changes of water vapour isotopes may be a key driver of variations in surface snow isotopes. Such control could explain how paleoclimate signals can be continuously recorded by water isotope variations in ice cores, even for periods without any precipitation. It has been suggested that a local diurnal cycle of sublimation and deposition could cause this isotope exchange between vapour and snow, but more detailed case studies and a combination of vapour and snow isotope data are required to better understand this process.

The performed moisture source diagnostics based on back-trajectory simulations show that the moisture origin for Neumayer Station depends on the season. With the frontal zone moving north in summer, moisture uptake for Neumayer is closer to the coast in summer, whereas in spring and fall the moisture has its origin in a wider region reaching farther north. However, the presented back-trajectory simulations are least reliable for cold periods due to a strong bias in the ERA-Interim data set concerning wind speed and the frequency of southerly winds. This particularly affects our analysis based on back-trajectory simulations when cold, dry and thus depleted air is advected from the continent. Also, the very high variability of surface pressure around Antarctica has to be considered, and a longer study period would be desirable in order to get more reliable results.

The Picarro measurements at Neumayer Station are currently being continued and supplemented by surface snow sampling. They will be used for a longer-term study in the future, which should also help to confirm and support the results of this study in more detail.

Appendix A: $\delta^{18}O$ vs. δD and d–excess

Appendix B: d–excess vs. temperature and humidity

https://doi.org/10.5194/tc-2020-302
Preprint. Discussion started: 27 October 2020

The Cryosphere Discussions
Open Access
EGU

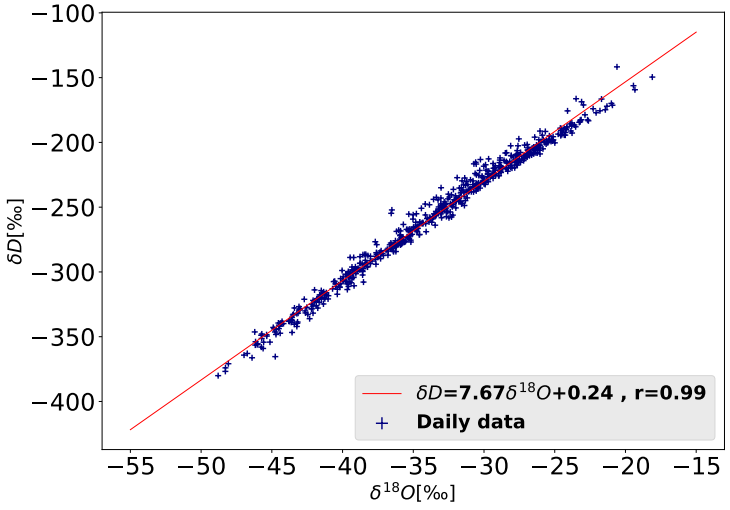

Figure A1. Daily averaged observed $\delta^{18}O$ [‰] vs. δD [‰] at Neumayer Station from February 2017 to January 2019. A best fitted line, using the least-squares approach, is plotted as a red line and corresponding correlation coefficients are calculated.

https://doi.org/10.5194/tc-2020-302
Preprint. Discussion started: 27 October 2020

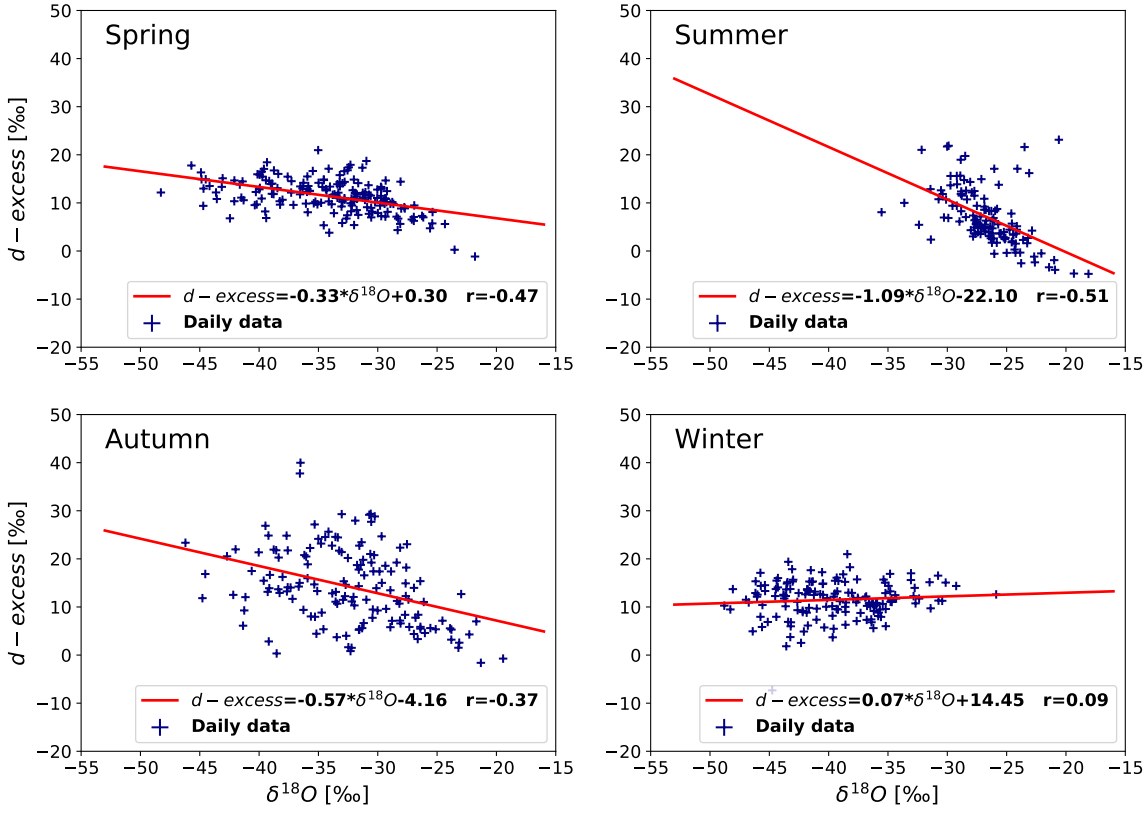

Figure A2. Deuterium excess [‰] vs. $\delta^{18}O$ [‰]. Four plots show daily average $\delta^{18}O$-d–excess values for different seasons of the year. For each season, a best fitted line, using the least-squares approach, for d–excess vs. $\delta^{18}O$ is plotted as a red line and corresponding correlation coefficients are calculated.

https://doi.org/10.5194/tc-2020-302
Preprint. Discussion started: 27 October 2020

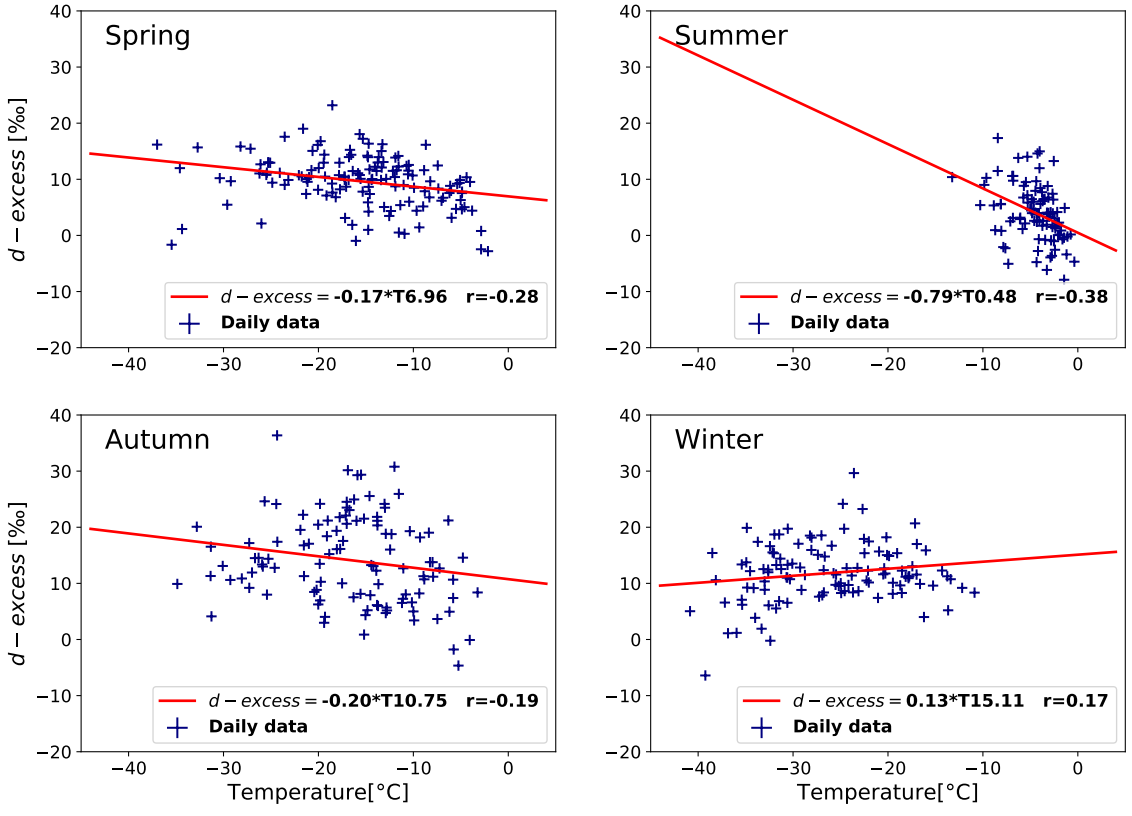

Figure B1. As Fig. A2, but for d–excess [‰] vs. temperature [°C].

https://doi.org/10.5194/tc-2020-302
Preprint. Discussion started: 27 October 2020

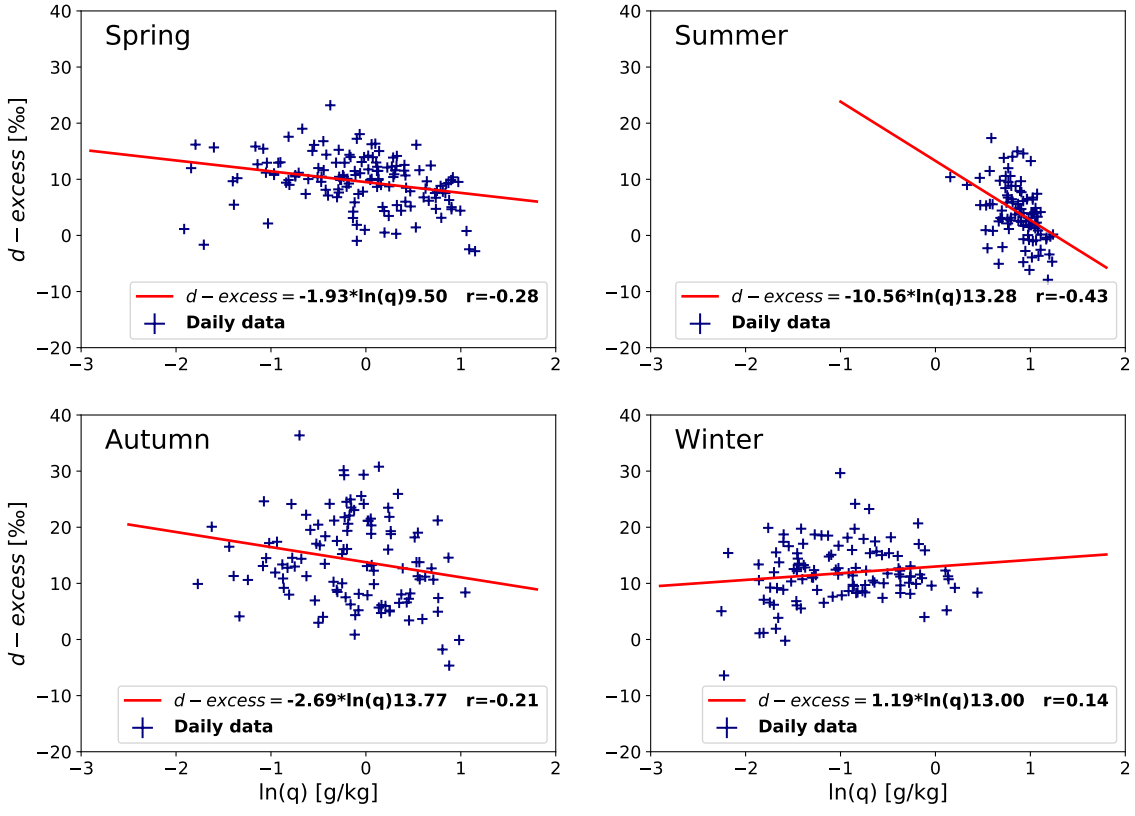

Figure B2. As Fig. A2, but for d–excess [‰] vs. natural logarithmic humidity [$g\ kg^{-1}$].

https://doi.org/10.5194/tc-2020-302
Preprint. Discussion started: 27 October 2020

References

Bonne, J.-L., Masson-Delmotte, V., Cattani, O., Delmotte, M., Risi, C., Sodemann, H., and Steen-Larsen, H. C.: The isotopic composition of water vapour and precipitation in Ivittuut, southern Greenland, Atmos. Chem. Phys., 14, 4419–4439, https://doi.org/10.5194/acp-14-4419-2014, 2014.

Bréant, C., Dos Santos, C. L., Agosta, C., Casado, M., Fourré, E., Goursaud, S., Masson-Delmotte, V., Favier, V., Cattani, O., Prié, F., et al.: Coastal water vapor isotopic composition driven by katabatic wind variability in summer at Dumont d'Urville, coastal East Antarctica, Earth Planet Sc. Lett., 514, 37–47, https://doi.org/10.1016/j.epsl.2019.03.004, 2019.

Brioude, J., Arnold, D., Stohl, A., Cassiani, M., Morton, D., Seibert, P., Angevine, W., Evan, S., Dingwell, A., Fast, J. D., Easter, R. C., Pisso, I., Burkhart, J., and Wotawa, G.: The Lagrangian particle dispersion model FLEXPART-WRF version 3.1, Geosci. Model Dev., 6, 1889–1904, https://doi.org/10.5194/gmd-6-1889-2013, 2013.

Buizert, C., Adrian, B., Ahn, J., Albert, M., Alley, R. B., Baggenstos, D., Bauska, T. K., Bay, R. C., Bencivengo, B. B., Bentley, C. R., Brook, E. J., Chellman, N. J., Clow, G. D., Cole-Dai, J., Conway, H., Cravens, E., Cuffey, K. M., Dunbar, N. W., Edwards, J. S., Fegyveresi, J. M., Ferris, D. G., Fitzpatrick, J. J., Fudge, T. J., Gibson, C. J., Gkinis, V., Goetz, J. J., Gregory, S., Hargreaves, G. M., Iverson, N., Johnson, J. A., Jones, T. R., Kalk, M. L., Kippenhan, M. J., Koffman, B. G., Kreutz, K., Kuhl, T. W., Lebar, D. A., Lee, J. E., Marcott, S. A., Markle, B. R., Maselli, O. J., McConnell, J. R., McGwire, K. C., Mitchell, L. E., Mortensen, N. B., Neff, P. D., Nishiizumi, K., Nunn, R. M., Orsi, A. J., Pasteris, D. R., Pedro, J. B., Pettit, E. C., Buford Price, P., Priscu, J. C., Rhodes, R. H., Rosen, J. L., Schauer, A. J., Schoenemann, S. W., Sendelbach, P. J., Severinghaus, J. P., Shturmakov, A. J., Sigl, M., Slawny, K. R., Souney, J. M., Sowers, T. A., Spencer, M. K., Steig, E. J., Taylor, K. C., Twickler, M. S., Vaughn, B. H., Voigt, D. E., Waddington, E. D., Welten, K. C., Wendricks, A. W., White, J. W. C., Winstrup, M., Wong, G. J., Woodruff, T. E., and Members, W. D. P.: Precise interpolar phasing of abrupt climate change during the last ice age, Nature, 520, 661–665, https://doi.org/10.1038/nature14401, 2015.

Casado, M., LANDAIS, A., Masson-Delmotte, V., Genthon, C., Kerstel, E., Kassi, S., Arnaud, L., Picard, G., Prie, F., Cattani, O., Steen-Larsen, H.-C., Vignon, E., and Cermak, P.: Continuous measurements of isotopic composition of water vapour on the East Antarctic Plateau, Atmos. Chem. Phys., 16, 8521–8538, https://doi.org/10.5194/acp-16-8521-2016, 2016.

Casado, M., Orsi, A., and Landais, A.: On the limits of climate reconstruction from water stable isotopes in polar ice cores, PAGES Magazine, 25, 146–147, https://doi.org/10.22498/pages.25.3.146, 2017.

Casado, M., Landais, A., Picard, G., Münch, T., Laepple, T., Stenni, B., Dreossi, G., Ekaykin, A., Arnaud, L., Genthon, C., Touzeau, A., Masson-Delmotte, V., and Jouzel, J.: Archival processes of the water stable isotope signal in East Antarctic ice cores, The Cryosphere, 12, 1745–1766, https://doi.org/10.5194/tc-12-1745-2018, 2018.

Dansgaard, W.: Stable isotopes in precipitation, Tellus, 16, 436–468, 1964.

Dee, D. P., Uppala, S. M., Simmons, A. J., Berrisford, P., Poli, P., Kobayashi, S., Andrae, U., Balmaseda, M. A., Balsamo, G., Bauer, P., Bechtold, P., Beljaars, A. C. M., van de Berg, L., Bidlot, J., Bormann, N., Delsol, C., Dragani, R., Fuentes, M., Geer, A. J., Haimberger, L., Healy, S. B., Hersbach, H., Hólm, E. V., Isaksen, L., Kållberg, P., Köhler, M., Matricardi, M., McNally, A. P., Monge-Sanz, B. M., Morcrette, J.-J., Park, B.-K., Peubey, C., de Rosnay, P., Tavolato, C., Thépaut, J.-N., and Vitart, F.: The ERA-Interim reanalysis: configuration and performance of the data assimilation system, Q. J. Roy. Meteor. Soc., 137, 553–597, https://doi.org/10.1002/qj.828, 2011.

EPICA Members: Nature, 429, 623–628, https://doi.org/10.1038/nature02599, 2004.

https://doi.org/10.5194/tc-2020-302
Preprint. Discussion started: 27 October 2020

Fernandoy, F., Meyer, H., Oerter, H., Wilhelms, F., Graf, W., and Schwander, J.: Temporal and spatial variation of stable-isotope ratios and accumulation rates in the hinterland of Neumayer Station, East Antarctica, J. Glaciol., 56, 673–687, https://doi.org/10.3189/002214310793146296, 2010.

Helsen, M., Van de Wal, R., Van den Broeke, M., As, D. v., Meijer, H., and Reijmer, C.: Oxygen isotope variability in snow from western Dronning Maud Land, Antarctica and its relation to temperature, Tellus B., 57, 423–435, https://doi.org/10.3402/tellusb.v57i5.16563, 2005.

Jouzel, J. and Merlivat, L.: Deuterium and oxygen 18 in precipitation: Modeling of the isotopic effects during snow formation, J. Geophys. Res. Atmos., 89, 11 749–11 757, https://doi.org/10.1029/JD089iD07p11749, 1984.

Jouzel, J., Masson-Delmotte, V., Cattani, O., Dreyfus, G., Falourd, S., Hoffmann, G., Minster, B., Nouet, J., Barnola, J. M., Chappellaz, J., Fischer, H., Gallet, J. C., Johnsen, S., Leuenberger, M., Loulergue, L., Luethi, D., Oerter, H., Parrenin, F., Raisbeck, G., Raynaud, D., Schilt, A., Schwander, J., Selmo, E., Souchez, R., Spahni, R., Stauffer, B., Steffensen, J. P., Stenni, B., Stocker, T. F., Tison, J. L., Werner, M., and Wolff, E. W.: Orbital and Millennial Antarctic Climate Variability over the Past 800,000 Years, Science, 317, 793–796, https://doi.org/10.1126/science.1141038, 2007.

Kerstel, E. T., Van Trigt, R., Reuss, J., and Meijer, H.: Simultaneous determination of the $^{2}H/^{1}H$, $^{17}O/^{16}O$, and $^{18}O/^{16}O$ isotope abundance ratios in water by means of laser spectrometry, Anal. Chem., 71, 5297–5303, https://doi.org/10.1021/ac990621e, 1999.

Klöwer, M., Jung, T., König-Langlo, G., and Semmler, T.: Aspects of weather parameters at Neumayer Station, Antarctica, and their representation in reanalysis and climate model data, Meteorol. Z., 22, 699–709, https://doi.org/10.1127/0941-2948/2013/0505, 2013.

König-Langlo, G.: Basic and other measurements, and meteorological synoptical observations from Neumayer Station, 1992-04 to 2016-01, reference list of 572 datasets, https://doi.org/10.1594/PANGAEA.874984, 2017.

König-Langlo, G. and Loose, B.: The meteorological observatory at Neumayer Stations (GvN and NM-II) Antarctica, Polarforschung2006, 76, 25–38, 2007.

Kurita, N., Hirasawa, N., Koga, S., Matsushita, J., Steen-Larsen, H. C., Masson-Delmotte, V., and Fujiyoshi, Y.: Influence of large-scale atmospheric circulation on marine air intrusion toward the East Antarctic coast, Geophys. Res. Lett., 43, 9298–9305, https://doi.org/10.1002/2016GL070246, 2016.

Lee, X., Sargent, S., Smith, R., and Tanner, B.: In situ measurement of the water vapor $^{18}O/^{16}O$ isotope ratio for atmospheric and ecological applications, J. Atmos. Ocean Tech., 22, 555–565, https://doi.org/10.1175/JTECH1719.1, 2005.

Lorius, C. and Merlivat, L.: Distribution of mean surface stable isotopes values in East Antarctica; observed changes with depth in coastal area, Tech. rep., CEA Centre d'Etudes Nucleaires de Saclay, 1975.

Loulergue, L., Schilt, A., Spahni, R., Masson-Delmotte, V., Blunier, T., Lemieux, B., Barnola, J.-M., Raynaud, D., Stocker, T. F., and Chappellaz, J.: Orbital and millennial-scale features of atmospheric CH_4 over the past 800,000 years, Nature, 453, 383–386, https://doi.org/10.1038/nature06950, 2008.

Lüthi, D., Le Floch, M., Bereiter, B., Blunier, T., Barnola, J.-M., Siegenthaler, U., Raynaud, D., Jouzel, J., Fischer, H., Kawamura, K., et al.: High-resolution carbon dioxide concentration record 650,000–800,000 years before present, Nature, 453, 379–382, https://doi.org/10.1038/nature06949, 2008.

Madsen, M. V., Steen-Larsen, H. C., Hörhold, M., Box, J., Berben, S. M. P., Capron, E., Faber, A.-K., Hubbard, A., Jensen, M. F., Jones, T. R., Kipfstuhl, S., Koldtoft, I., Pillar, H. R., Vaughn, B. H., Vladimirova, D., and Dahl-Jensen, D.: Evidence of Isotopic Fractionation During Vapor Exchange Between the Atmosphere and the Snow Surface in Greenland, J. Geophys. Res. Atmos., 124, 2932–2945, https://doi.org/10.1029/2018JD029619, 2019.

Masson-Delmotte, V., Kageyama, M., Braconnot, P., Charbit, S., Krinner, G., Ritz, C., Guilyardi, E., Jouzel, J., Abe-Ouchi, A., Crucifix, M., et al.: Past and future polar amplification of climate change: climate model intercomparisons and ice-core constraints, Clim. Dynam., 26, 513–529, https://doi.org/10.1007/s00382-005-0081-9, 2006.

Masson-Delmotte, V., Hou, S., Ekaykin, A., Jouzel, J., Aristarain, A., Bernardo, R. T., Bromwich, D., Cattani, O., Delmotte, M., Falourd, S., Frezzotti, M., Gallée, H., Genoni, L., Isaksson, E., Landais, A., Helsen, M. M., Hoffmann, G., Lopez, J., Morgan, V., Motoyama, H., Noone, D., Oerter, H., Petit, J. R., Royer, A., Uemura, R., Schmidt, G. A., Schlosser, E., Simões, J. C., Steig, E. J., Stenni, B., Stievenard, M., van den Broeke, M. R., van de Wal, R. S. W., van de Berg, W. J., Vimeux, F., and White, J. W. C.: A Review of Antarctic Surface Snow Isotopic Composition: Observations, Atmospheric Circulation, and Isotopic Modeling, J. Climate, 21, 3359–3387, https://doi.org/10.1175/2007JCLI2139.1, 2008.

Masson-Delmotte, V., Buiron, D., Ekaykin, A., Frezzotti, M., Gallee, H., Jouzel, J., Krinner, G., Landais, A., Motoyama, H., Oerter, H., Pol, K., Pollard, D., Ritz, C., Schlosser, E., Sime, L. C., Sodemann, H., Stenni, B., Uemura, R., and Vimeux, F.: A comparison of the present and last interglacial periods in six Antarctic ice cores, Clim. Past, 7, 397–423, https://doi.org/10.5194/cp-7-397-2011, 2011.

Medley, B., McConnell, J. R., Neumann, T. A., Reijmer, C. H., Chellman, N., Sigl, M., and Kipfstuhl, S.: Temperature and Snowfall in Western Queen Maud Land Increasing Faster Than Climate Model Projections, Geophys. Res. Lett., 45, 1472–1480, https://doi.org/10.1002/2017GL075992, 2018.

Merlivat, L. and Jouzel, J.: Global climatic interpretation of the deuterium-oxygen 18 relationship for precipitation, J. Geophys. Res. Oceans, 84, 5029–5033, https://doi.org/10.1029/JC084iC08p05029, 1979.

Münch, T., Kipfstuhl, S., Freitag, J., Meyer, H., and Laepple, T.: Regional climate signal vs. local noise: a two-dimensional view of water isotopes in Antarctic firn at Kohnen station, Dronning Maud Land, Clim. Past., 12, 1565–1581, https://doi.org/10.5194/cp-12-1565-2016, 2016.

Petit, J. R., Jouzel, J., Raynaud, D., Barkov, N. I., Barnola, J. M., Basile, I., Bender, M., Chappellaz, J., Davis, M., Delaygue, G., Delmotte, M., Kotlyakov, V. M., Legrand, M., Lipenkov, V. Y., Lorius, C., PÉpin, L., Ritz, C., Saltzman, E., and Stievenard, M.: Climate and atmospheric history of the past 420,000 years from the Vostok ice core, Antarctica, Nature, 399, 429–436, https://doi.org/10.1038/20859, 1999.

Pfahl, S. and Sodemann, H.: What controls deuterium excess in global precipitation?, Clim. Past, 10, 771–781, https://doi.org/10.5194/cp-10-771-2014, 2014.

Pfahl, S., Wernli, H., and Yoshimura, K.: The isotopic composition of precipitation from a winter storm: a case study with the limited-area model COSMOiso, Atmos. Chem. Phys., 12, 1629–1648, https://doi.org/doi:10.5194/acp-12-1629-2012, 2012.

Rimbu, N., Lohmann, G., König-Langlo, G., Necula, C., and Ionita, M.: Daily to intraseasonal oscillations at Antarctic research station Neumayer, Antarct. Sci., 26, 193–204, https://doi.org/10.1017/S0954102013000540, 2014.

Risi, C., Bony, S., Vimeux, F., and Jouzel, J.: Water-stable isotopes in the LMDZ4 general circulation model: Model evaluation for present-day and past climates and applications to climatic interpretations of tropical isotopic records, J. Geophys. Res. Atmos., 115, https://doi.org/10.1029/2009JD013255, 2010.

Ritter, F., Steen-Larsen, H. C., Werner, M., Masson-Delmotte, V., Orsi, A., Behrens, M., Birnbaum, G., Freitag, J., Risi, C., and Kipfstuhl, S.: Isotopic exchange on the diurnal scale between near-surface snow and lower atmospheric water vapor at Kohnen station, East Antarctica, The Cryosphere, 10, 1647–1663, https://doi.org/10.5194/tc-10-1647-2016, 2016.

https://doi.org/10.5194/tc-2020-302
Preprint. Discussion started: 27 October 2020

Salamatin, A. N., Lipenkov, V. Y., Barkov, N. I., Jouzel, J., Petit, J. R., and Raynaud, D.: Ice core age dating and paleothermometer calibration based on isotope and temperature profiles from deep boreholes at Vostok Station (East Antarctica), J. Geophys. Res. Atmos., 103, 8963–8977, https://doi.org/10.1029/97JD02253, 1998.

Schlosser, E., Reijmer, C., Oerter, H., and Graf, W.: The influence of precipitation origin on the $\delta^{18}O$–T relationship at Neumayer Station, Ekstrmisen, Antarctica, Ann. Glaciol., 39, 41–48, https://doi.org/10.3189/172756404781814276, 2004.

Schmithüsen, H., König-Langlo, G., Müller, H., and Schulz, H.: Continuous meteorological observations at Neumayer Station (2010-2018), reference list of 108 datasets, https://doi.org/10.1594/PANGAEA.908826, 2019.

Siegenthaler, U., Stocker, T. F., Monnin, E., Lüthi, D., Schwander, J., Stauffer, B., Raynaud, D., Barnola, J.-M., Fischer, H., Masson-Delmotte, V., and Jouzel, J.: Stable Carbon Cycle–Climate Relationship During the Late Pleistocene, Science, 310, 1313–1317, https://doi.org/10.1126/science.1120130, 2005.

Sime, L., Wolff, E., Oliver, K., and Tindall, J.: Evidence for warmer interglacials in East Antarctic ice cores, Nature, 462, 342–345, https://doi.org/10.1038/nature08564, 2009.

Sime, L. C., Risi, C., Tindall, J. C., Sjolte, J., Wolff, E. W., Masson-Delmotte, V., and Capron, E.: Warm climate isotopic simulations: what do we learn about interglacial signals in Greenland ice cores?, Quaternary Sci. Rev., 67, 59–80, https://doi.org/10.1016/j.quascirev.2013.01.009, 2013.

Sodemann, H., Masson-Delmotte, V., Schwierz, C., Vinther, B. M., and Wernli, H.: Interannual variability of Greenland winter precipitation sources: 2. Effects of North Atlantic Oscillation variability on stable isotopes in precipitation, J. Geophys. Res. Atmos., 113, https://doi.org/10.1029/2007JD009416, 2008.

Steen-Larsen, H., Masson-Delmotte, V., Hirabayashi, M., Winkler, R., Satow, K., Prié, F., Bayou, N., Brun, E., Cuffey, K., Dahl-Jensen, D., Dumont, M., Guillevic, M., Kipfstuhl, S., Landais, A., Popp, T., Risi, C., Steffen, K., Stenni, B., and Sveinbjörnsdottír, A.: What controls the isotopic composition of Greenland surface snow?, Clim. Past, 10, 377–392, 2014.

Steen-Larsen, H. C., Johnsen, S. J., Masson-Delmotte, V., Stenni, B., Risi, C., Sodemann, H., Balslev-Clausen, D., Blunier, T., Dahl-Jensen, D., Ellehøj, M. D., Falourd, S., Grindsted, A., Gkinis, V., Jouzel, J., Popp, T., Sheldon, S., Simonsen, S. B., Sjolte, J., Steffensen, J. P., Sperlich, P., Sveinbjörnsdóttir, A. E., Vinther, B. M., and White, J. W. C.: Continuous monitoring of summer surface water vapor isotopic composition above the Greenland Ice Sheet, Atmos. Chem. Phys., 13, 4815–4828, https://doi.org/10.5194/acp-13-4815-2013, 2013.

Werner, M., Langebroek, P. M., Carlsen, T., Herold, M., and Lohmann, G.: Stable water isotopes in the ECHAM5 general circulation model: Toward high-resolution isotope modeling on a global scale, J. Geophys. Res. Atmos., 116, https://doi.org/10.1029/2011JD015681, 2011.

Werner, M., Jouzel, J., Masson-Delmotte, V., and Lohmann, G.: Reconciling glacial Antarctic water stable isotopes with ice sheet topography and the isotopic paleothermometer, Nat. Commun., 9, 1–10, https://doi.org/10.1038/s41467-018-05430-y, 2018.

Competing interests.

We have no conflicts of interest to disclose.

Acknowledgements. This work was funded by the Helmholtz Climate Initiative REKLIM (Regional Climate Change), a joint research initiative of the Helmholtz Association of German research centres (HGF).